East-west extension in the NW Indian Himalaya

Esther Hintersberger[1,*], Rasmus Ch. Thiede[1,†], Manfred R. Strecker[1,§], and Bradley R. Hacker[2,#]
[1]*Institut für Geowissenschaften, Universität Potsdam, Karl-Liebknecht-Strasse 24, 14476 Potsdam, Germany*
[2]*Institute for Crustal Studies, University of California, Santa Barbara, California 93106-9630, USA*

ABSTRACT

Explaining the presence of normal faults in overall compressive settings is a challenging problem in understanding the tectonics of active mountain belts. The Himalayan-Tibetan orogenic system is an excellent setting to approach this problem because it preserves one of the most dramatic records of long-term, contemporaneous shortening and extension. Over the past decades, several studies have described extensional features, not only in the Tibetan Plateau, but also in the Himalaya. For a long time, the favored model explained the function of the Southern Tibetan detachment system, a major fault zone in the Himalaya, as a decoupling horizon between the regime of crustal shortening forming the Himalayan wedge to the south and the extensional regime of the Tibetan Plateau to the north. However, in recent years, increasing evidence has shown that N-S–trending normal faults in the Central Himalaya crosscut not only the Southern Tibetan detachment system, but also the Main Central thrust.

Here, we present new structural data and geologic evidence collected within the NW Indian Himalaya and combine them with previously published seismicity data sets in order to document pervasive E-W extension accommodated along N-S–trending faults extending as far south as the footwall of the Main Central thrust. We conducted a kinematic analysis of fault striations on brittle faults, documented and mapped fault scarps in Quaternary sedimentary deposits using satellite imagery, and made field observations in the Greater Sutlej region (Spiti, Lahul, Kinnaur) and the Garhwal Himalaya. Studies of extensional features within the regionally NW-SE–trending NW Indian Himalaya provide the advantage that arc-parallel and E-W extension can be separated, in contrast to the Central Himalaya. Therefore, our observations of E-W extension in the Indian NW Himalaya are well suited to test the applicability of current tectonic models for the whole Himalaya. We favor the interpretation of E-W extension in the NW Indian Himalaya as a propagation of extension driven by collapse of the Tibetan Plateau.

INTRODUCTION

The mechanistic principle governing the spatial-temporal evolution of normal fault systems in active mountain belts is still a matter of dispute (e.g., Kapp and Guynn, 2004; Selverstone, 2005; Murphy et al., 2009). Observations in Cenozoic orogens related to continent-continent collision like the Himalaya-Tibet region (e.g., Armijo et al., 1986; Molnar, 1992; Chen and Yang, 2004; Zhang et al., 2004), the Pamir (e.g., Burtman and Molnar, 1993; Strecker et al., 1995), or the Alps (e.g., Michard et al., 1993; Wheeler and Butler, 1993; Seward and Mancktelow, 1994; Selverstone, 2005; Sue et al., 2007) document extension and normal faulting occurring contemporaneously at higher elevations, with shortening and thrusting occurring at lower elevations.

Various mechanisms attempting to explain this high-elevation normal faulting have been proposed. In the transition between the Himalaya and Tibet region, the generation of normal faults parallel to the trend of the orogen, e.g., the Southern Tibetan detachment system (Burg et al., 1984; Burchfiel et al., 1992), has been explained by processes associated with channel flow or extrusion of the orogenic wedge (e.g., Grujic et al., 1996; Nelson et al., 1996; Beaumont et al., 2001; Vannay and Grasemann, 2001). Other explanations include the increase of potential gravitational energy, followed by collapse due to excess elevation (e.g., Royden and Burchfiel, 1987; Buck and Sokoutis, 1994; Hodges et al., 2001), basal shear produced by southward crustal flow below the Himalaya (Yin, 1989), and, more recently, a passive roof-thrust model (Yin, 2006; Webb et al., 2007).

Models that have been invoked to explain orogen-perpendicular grabens of the Himalaya and the southern Tibetan Plateau include an additional variety of mechanisms. The most prominent ones include (1) radial thrusting (e.g., Seeber and Armbruster, 1984; Armijo et al., 1986; Molnar and Lyon-Caen, 1989); (2) oroclinal bending (e.g., Ratschbacher et al., 1994; Kapp and Yin, 2001; Robinson et al., 2007); (3) partitioning of oblique convergence into thrusting and normal faulting components (e.g., McCaffrey, 1996; McCaffrey and Nabelek, 1998); (4) southward propagation of the subduction front (Murphy and Copeland, 2005); (5) concentrated compression at the Central Himalayan front (Kapp and Guynn, 2004); (6) change of boundary conditions along the eastern margin of Asia (Yin, 2000; Yin and Harrison, 2000); (7) convective removal of the mantle lithosphere (England and Houseman, 1989); and finally, (8) those models linked with escape tectonics in the course of the continental collision process (e.g., Molnar and Tapponnier, 1978; Tapponnier et al., 1982; Molnar and Chen, 1983; Royden and Burchfiel, 1987). In general, these models can be combined into two major groups: the first one contains all models where extension is related to processes within the Himalaya and the arcuate shape of the orogen, such as oroclinal bending, and radial thrusting. The second group relates extension to deeper-seated processes, mainly within the Tibetan Plateau.

The Himalayan collision zone, which is characterized by ongoing shortening due to the convergence of India and Eurasia, hosts major active normal fault systems that strike approximately perpendicular to the trend of the orogen (Armijo et al., 1986; Royden and Burchfiel, 1987; Molnar and Lyon-Caen, 1989; Burchfiel et al., 1991; Ratschbacher et al., 1994; McCaffrey and Nabelek, 1998; Hodges et al., 2001; Murphy et al., 2002; Aoya et al., 2005; Thiede et al., 2006). Global positioning system (GPS) measurements

*E-mail: estherh@geo.uni-potsdam.de
†Current address: ETH Zürich, Geologisches Institut, NO E 45, Sonneggstrasse 5, 8092 Zürich, Switzerland; e-mail: rasmus.thiede@erdw.ethz.ch
§E-mail: strecker@geo.uni-potsdam.de
#E-mail: hacker@geol.ucsb.edu

GSA Bulletin; September/October 2010; v. 122; no. 9/10; p. 1499–1515; doi: 10.1130/B26589.1; 11 figures; 3 tables; Data Repository item 2010128.

and fault-plane solutions of earthquakes indicate approximately radial shortening in the Himalaya and E-W extension in the Tibetan Plateau (Zhang et al., 2004; Molnar and Lyon-Caen, 1989). However, in the central part of the Himalaya between 84°E and 92°E longitude, tectonism does not conform to this first-order kinematic differentiation. In this high-relief region, with mean elevations of ~3000 m, numerous N-S–striking extensional fractures, closely spaced normal faults, and linked graben systems document extensional processes that are not limited to the Tibetan Plateau and the internal parts of Himalaya, but that also affect the high Himalayan realm farther south. Crosscutting relationships indicate that these extensional structures cut all preexisting deformation fabrics and structures, including older, orogen-parallel normal faults. This is documented by observations in the vicinity of the Gurla Mandhata gneiss dome and around the Ama Drime Massif (e.g., Murphy and Copeland, 2005; Jessup et al., 2008). The driving forces for their generation, whether they are rooted in the geometry of the Himalaya or in the eastward motion of the Tibetan Plateau, are still an open question, mainly because in the Central Himalaya, both extensional directions are oriented approximately E-W.

In this paper, we take advantage of the regionally NW-SE–oriented strike of the orogen in the NW Indian Himalaya to differentiate between extension triggered within the Himalaya and extensional processes triggered by deformation of Tibetan Plateau. We present new field evidence from structural mapping, analysis of satellite imagery (ASTER, GoogleEarth, LandSat), and new fault kinematic data from brittle faults from the NW Indian Himalaya. We document normal faulting that is not simply localized in close vicinity to major structures, but rather is a ubiquitous, pervasive phenomenon affecting the NW India Himalaya as a whole. Our new data help define the spatial-temporal character of the extensional deformation and provide valuable information on the causal mechanisms of active normal faulting of the studied region. Our data set shows that extension is not limited to the higher parts of the Himalaya, but it is also found in the lower-elevation regions, with average elevations of around 1500 m, in the foreland of the Main Central thrust.

Because previous models explaining the origin of extension in the Himalaya have been generally based on data from the Central Himalaya, we used our new observations from the NW sector of the orogen to evaluate those models. Based on this evaluation, we favor a scenario where E-W–oriented extension in the NW Indian Himalaya is triggered by extension in the Tibetan Plateau.

GEOLOGICAL SETTING OF THE NW HIMALAYA

Principal Structures Related to Shortening

In the NW Himalaya, the curved orogen trends dominantly NW-SE and can be separated into five principal lithologic-tectonic provinces, including the Sub-Himalaya, the Lesser Himalaya, the Higher Himalaya, and the Tethyan Himalaya (Gansser, 1964). These tectonic provinces are fault bounded and accommodate ~30%–50% of India-Eurasia plate convergence (Banerjee and Bürgmann, 2002; Zhang et al., 2004). The NW Himalaya has accommodated SSW-directed shortening and thrusting caused by the underthrusting of India beneath Eurasia since the collision at around 55 Ma (Klootwijk et al., 1985). This process has been associated with a stepwise southward migration of thrust systems, from the Main Central thrust (since 23–20 Ma; Hodges et al., 1996) to the Main Boundary thrust (since 11–9 Ma; Meigs et al., 1995) to the Main Frontal thrust, which has been active since the Pliocene (Molnar, 1984; Wesnousky et al., 1999). In addition to these structures, in the NW Himalaya, the ductile, north-dipping Munsiari thrust (MT) between the Main Central thrust and the Main Boundary thrust separates the Lesser Himalayan crystalline sequence from the Lesser Himalayan paragneisses (Fig. 1B; Vannay et al., 2004).

Extensional Structures in the Himalaya

Contemporaneous with crustal shorting along the southern mountain front, large regions of the Himalaya are characterized by activity along orogen-parallel and orogen-perpendicular normal faults (e.g., Le Fort et al., 1982; Burchfiel et al., 1992; Wu et al., 1998). One of the extensional hallmarks of the Himalaya is the system of orogen-parallel, linked normal faults associated with the Southern Tibetan detachment system. The Southern Tibetan detachment system strikes parallel to major thrusts and separates the low-grade metamorphic rocks of the Tethyan Himalaya in the hanging wall from the high-grade metamorphic footwall of the Higher Himalaya (Burg et al., 1984; Burchfiel and Royden, 1985; Burchfiel et al., 1992). During the Miocene, the Higher Himalaya was exhumed during coeval extension along the Southern Tibetan detachment system and thrusting along the Main Central thrust. Some studies have proposed that the Southern Tibetan detachment system has been reactivated as recently as the Quaternary (Hodges et al., 2001; Hurtado et al., 2001).

In the NW Indian Himalaya, the Sangla detachment is the local expression of the Southern Tibetan detachment system in the Greater Sutlej region (Vannay and Grasemann, 1998; Wiesmayr and Grasemann, 2002). This structure is well recognized in the field; however, evidence for neotectonic activity has not been observed by us or by several earlier investigations (e.g., Vannay and Grasemann, 1998). Recent studies in the vicinity of the Kullu Valley (Fig. 1B) suggest that the Southern Tibetan detachment system and the Main Central thrust merge in map view, which the authors explain with a passive roof-thrust model for the development of the Southern Tibetan detachment system (Yin, 2006; Webb et al., 2007). In the Sutlej Valley, the brittle Karcham normal fault crosscuts the Main Central thrust mylonites, showing a top-to-the-east displacement, and it is assumed to have been the counterpart of the Munsiari thrust during the exhumation of the Lesser Himalayan crystalline sequence (Janda et al., 2002; Vannay et al., 2004). Other extensional detachments include the Leo Pargil detachment zone (Thiede et al., 2006) farther north and the Gurla Mandhata detachment zone (Murphy et al., 2000, 2002) farther east (Fig. 1), which form the low-angle ductile normal faults of two major domes exhumed during the Miocene in the Tethyan Himalaya.

A second group of extensional structures are made up of N-S–striking normal faults. In the NW Himalaya, several N-S–striking, high-angle brittle normal faults are documented in the vicinity of the Gurla Mandhata dome (Murphy et al., 2000, 2002), the Kaurik-Chango normal fault at the western flank of the Leo Pargil dome (Hayden, 1904; Thiede et al., 2006), and the Tso Kar and Tso Morari normal faults north of the Spiti Valley (e.g., Steck et al., 1993; Fuchs and Linner, 1996; Epard and Steck, 2008). Also in the Central Himalaya, between 83°E and 90°E, several large-scale, Neogene normal faults strike perpendicular to the orogen (Fig. 1A). These include structures bounding the Thakkola graben (Le Fort et al., 1982; Garzione et al., 2000; Hurtado et al., 2001; Garzione et al., 2003), structures close to the Ama Drime Massif (Jessup et al., 2008; Cottle et al., 2009) in Tibet, and the southern end of the Yadong graben in Bhutan (Wu et al., 1998; Guo et al., 2008). Several of these offset the Southern Tibetan detachment system, especially the N-S–striking normal faults bounding the Ama Drime Massif in the Central Himalaya, which displace the Southern Tibetan detachment system for several kilometers and thus represent the youngest deformation phase (Jessup et al., 2008). However, the southern and the northern terminations of those normal faults are not yet fully documented. This raises the question of

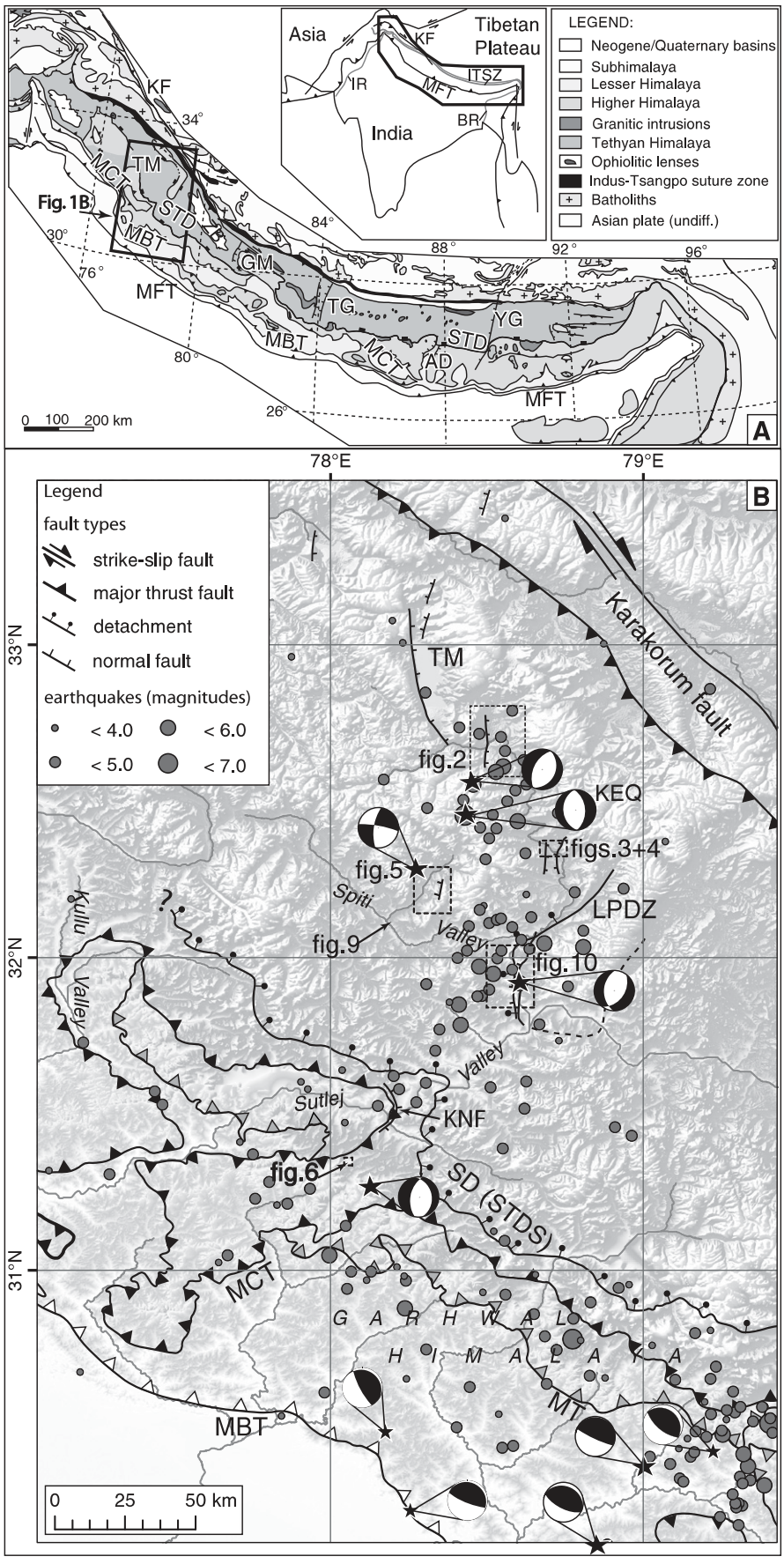

Figure 1. (A) Geological map and structural provinces of the entire Himalaya, modified after Yin (2006) and references therein. For the western Himalaya, the structures as mapped by DiPietro and Pogue (2004) are used. (B) Structural map of the NW Indian Himalaya, modified after Thiede et al. (2005, and references therein). Earthquakes, shown as dark-gray dots, are taken from the National Earthquake Information Center (NEIC) catalog; fault-plane solutions for the larger earthquakes are from the Harvard Centroid Moment Tensor (CMT) catalog. The fault-plane solution for the Kinnaur earthquake (KEQ) is labeled explicitly. Dotted rectangles represent the locations of figures shown later in the text. Locations of Figures 3 and 4 are too close to each other to be separated on this map scale; therefore, they are represented by one box. The base map shows elevations taken from a Shuttle Radar Topography Mission (SRTM) image. Abbreviations: AD—Ama Drime Massif, BR—Brahmaputra River, GM—Gurla Mandhata gneiss dome, IR—Indus River, ITSZ—Indus-Tsangpo suture zone, KEQ—Kinnaur earthquake, KF—Karakorum fault, KNF—Karcham normal fault, LPDZ—Leo Pargil detachment zone, MBT—Main Boundary thrust, MCT—Main Central thrust, MFT—Main Frontal thrust, MT—Munsiari thrust, SD—Sangla detachment, STDS—Southern Tibetan detachment system, TM—Tso Morari, TG—Thakkola graben, YG—Yadong graben, ZB—Zada Basin.

whether the N-S–striking grabens in the central and southern Tibetan Plateau are linked to the extensional processes observed within the Himalaya, or if they represent an entirely different, but possibly coeval process that generates very similar structures and geomorphic features that have their origin in the Tibetan Plateau.

Seismicity in the NW Indian Himalaya

Fault-plane solutions derived from seismicity in the Himalaya-Tibet region reflect first-order deformation patterns and provide insight into the characteristics of the present-day regional stress field (Fig. 1B). In the southern Tibetan Plateau, fault-plane solutions document pure normal faulting, indicating E-W extension, both at shallow crustal levels (<15 km) and at greater depths of 80–95 km (Molnar and Chen, 1983; Molnar and Lyon-Caen, 1989). In contrast, earthquakes in the Himalaya with radially oriented thrusting

focal mechanisms and magnitudes of up to 8.0 are located at depths between 20 and 40 km and are primarily related to the underthrusting of India beneath Eurasia (e.g., Seeber and Armbuster, 1981; Ni and Barazangi, 1984).

We extracted all seismic events of magnitude >3.2 recorded between 77.5°E and 79°E within the NW Indian Himalaya from the global seismicity catalogs (National Earthquake Information Center Catalog [NEIC], 2009; Harvard Global Centroid Moment Tensor [CMT] Catalog, 2009). This subset of seismic events can be separated into two groups. The southern Himalayan front is characterized by a group of large earthquakes with magnitudes up to M = 8.6 and dominant NE-SW shortening (Fig. 1B). Some of the most prominent examples are the Kangra (4 April 1905, M[estimated] = 8.6; Middlemiss, 1910), Uttarkashi (20 October 1991, Mw = 6.8; Kayal et al., 1992), and Chamoli earthquakes (29 March 1999, Mw = 6.6; Rastogi, 2000). The second group is characterized by shallow earthquakes with depths <15 km occupying a narrow swath between 78°E and 78.5°E, stretching from the Tso Morari dome in the north to close to the Main Central thrust in the south (Fig. 1B). The Kinnaur earthquake (19 January 1975, M_S = 6.8), with its epicentral zone close to the Leo Pargil gneiss dome, was the most prominent event of this group (fault-plane solution KEQ, see Fig. 1B). Fault-plane solutions for this event and other major earthquakes in the Sutlej region provide additional evidence for ongoing E-W extension (e.g., Molnar and Chen, 1983). The degree of activity in the Sutlej region is much higher than that recorded along other N-S–striking structures in the Himalaya, such as the Thakkola graben in Nepal, where only microseismicity with magnitudes <4 is observed (Pandey et al., 1999).

METHODOLOGY

Field Mapping and Analysis of Satellite Imagery

Previously, structures related to E-W extension have been only described around prominent morphologic features such as graben or dome systems. We were interested to see whether these extensional structures are restricted to these features, or if normal faulting is more pervasively distributed across the orogen. To explore this question, we collected structural field data on recent normal faults and interpreted satellite images from the Lesser and Higher Himalaya of NW India. We focused on an area extending from the Tso Morari dome in the north to the Garhwal Himalaya in the south, covering the region shown in Figure 1B.

We determined the kinematics of brittle faults in basement rocks and sedimentary strata, such as lake deposits and fluvial-terrace conglomerates. To better understand recent fault displacement, we analyzed fluvial terraces and paleosurfaces affected by Quaternary faulting (section: Macroscale Normal Faults from Satellite Imagery and Field Observations; Figs. 2–5). We used satellite imagery (LandSAT, ASTER, and GoogleEarth) where the border region between India and China did not permit direct field access. Detailed investigations of the fault inventory in river terraces were undertaken, such as in the immediate vicinity of the Leo Pargil gneiss dome and in the Spiti Valley (section: Normal Faults in Sediments and Soft-Sediment Deformation).

Kinematic Analysis of Brittle Fault Data

To obtain a better image of the distribution of paleo–strain axes in the study area, we collected fault kinematic data. We measured the strike and dip, slip direction, and sense of slip for

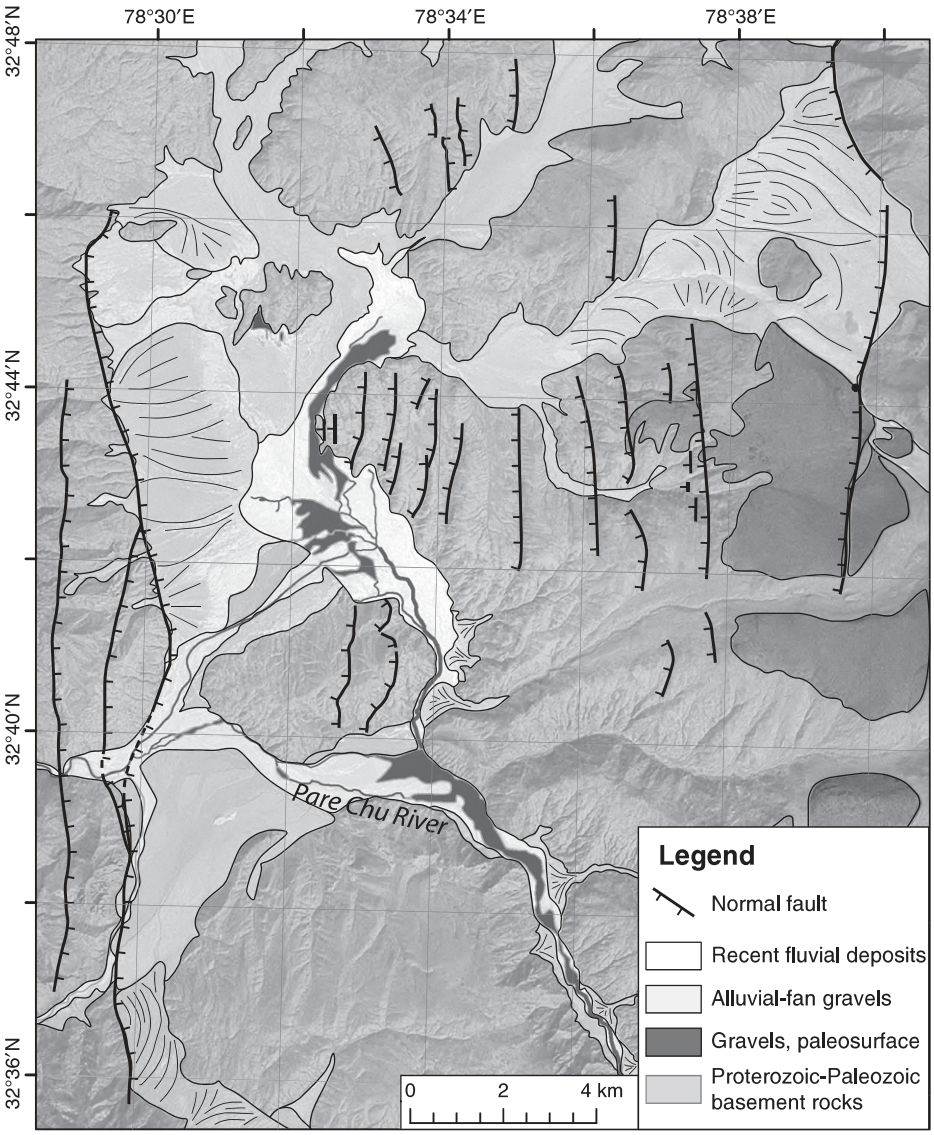

Figure 2. Normal faults mapped on a LandSat7-image of the region southeast of the Tso Morari Lake. In the west, the large east-dipping normal faults deform older alluvial fans. In the east, several smaller, antithetic normal faults dip toward the west and also affect an older paleosurface (dark gray). Both groups of normal faults have produced a half-graben system that influences the drainage system of the Pare Chu River. See Figure 1B for location.

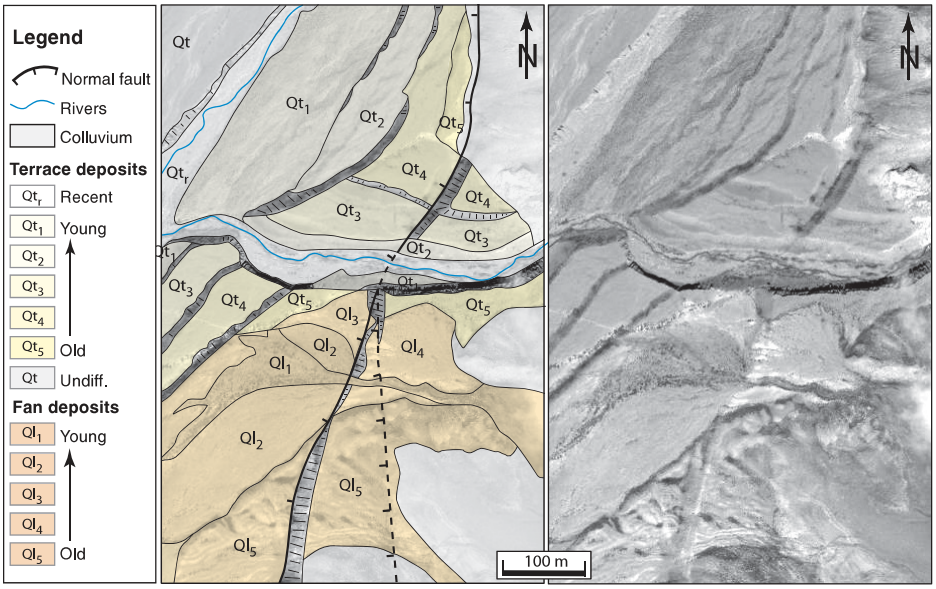

Figure 3. Example of Quaternary normal faulting in the NW Leo Pargil basin, where a normal fault displaces fluvial terraces (northern part) and alluvial fans (southern part). Terrace risers are marked with lines indicating the approximate slope direction. Uninterpreted GoogleEarth air-photo of this region is shown on the right. See Figure 1B for location.

major and minor brittle faults from the Spiti and Sutlej Valleys, the Kullu Valley, and the Garhwal Himalaya (see Fig. 1B). We selected only the youngest structures, which were mainly normal faults, and analyzed them with *Tectonics*FP (Ortner et al., 2002). For coaxial deformation, derived kinematic strain-axes can be interpreted carefully as paleo–stress axes. In the case of brittle faulting, the condition of coaxial deformation is met for fault planes outside of prominent shear zones. Therefore, we concentrated on outcrop-scale brittle faults with displacements of up to several centimeters. We used the kinematic P/T-axis method (P—pressure; T—tension; Turner, 1953), as well as the numeric dynamic analysis (NDA; Spang, 1972; Sperner, 1996) to cross-check differences introduced by the underlying assumptions. To compare our results with seismicity data, we generally assumed an angle of 45° between a fault plane and its P axis for the determination of P and T axes. The differences observed in the resultant extension and shortening directions from both methods were negligible, and were mostly within the limit of error.

Age Determination of Normal Faulting

We were able to constrain the minimum age for onset of normal faulting at three sites using $^{40}Ar/^{39}Ar$ and OSL (optically stimulated luminescence) techniques. South of the Leo Pargil gneiss dome, synkinematic micas on a fault plane were dated by the $^{40}Ar/^{39}Ar$ technique at the University of California in Santa Barbara. The mica separates were wrapped in Cu foil, sealed in a quartz vial, and irradiated at the TRIGA reactor at Oregon State University for 8 MW h. Ratios of reactor-produced Ca-derived isotopes were established by analyzing CaF_2 included in the irradiation vial. Sanidine from the Taylor Creek rhyolite, with an assumed age of 27.92 Ma, was used as a neutron flux monitor to determine the irradiation parameter, *J*. The samples were analyzed using a double-vacuum Staudacher-type resistance furnace in 12–15 min heating steps. Gas was gettered continuously during extraction with two SAES ST172 Zr-V-Fe getters. The collected gas was analyzed with an MAP-216 spectrometer using a Baur-Signer source and Johnston MM1 electron multiplier operating in static mode with a room temperature SAES ST707 Zr-V-Fe getter. Peak heights at the time of gas introduction into the mass spectrometer were determined by extrapolating the evolved signal size using a linear regression. Resistance furnace m/*e* 40 blanks varied from 2×10^{-16} moles at 800 °C to 6×10^{-16} moles at 1400 °C. Complete $^{40}Ar/^{39}Ar$ dating protocol is provided in the GSA Data Repository.[1]

[1]GSA Data Repository item 2010128, complete $^{40}Ar/^{39}Ar$ data set to Fig. 8 and Table 1, is available at http://www.geosociety.org/pubs/ft2009.htm or by request to editing@geosociety.org.

In addition, we took samples from Quaternary sedimentary deposits affected by normal faulting or layers subjected to soft-sediment deformation that may have been caused by coeval activity along nearby faults. These samples, collected in 20-cm-long, opaque tubes, were dated with the OSL technique. The analysis of the OSL samples was carried out by the Sheffield Centre for International Drylands Research (UK). The samples were prepared under subdued red lighting to extract and clean quartz following the procedure outlined in Bateman and Catt (1996). The remaining pure quartz, with grain sizes between 90 and 250 µm, was mounted as 4-mm-diameter aliquots and checked with infrared stimulated luminescence for feldspar contamination, which was not given. All OSL measurements were carried out using an upgraded DA-15 Risø luminescence reader system, equipped with a calibrated ^{90}Sr beta source and blue Light Emitting Diodes (LEDs) for stimulation. The OSL signal was measured through a Hoya-340 filter. All samples were analyzed using the single aliquot regenerative (SAR) approach (Murray and Wintle, 2000), where the last measurement replicated the first one. Aliquots were excluded from further analysis if the ratio of first and last dose point exceeded ±10% of unity. To remove unstable signals, the samples were preheated prior to OSL measurements using a preheat temperature of 180 °C for 10 s.

EXTENSIONAL STRUCTURES IN THE NW HIMALAYA

Here, we report on different phenomena related to normal faulting in the NW Indian Himalaya, where the deeply incised Sutlej and Spiti Rivers provide an excellent and easily accessible natural transect through the entire mountain range. Apart from the structures already mentioned here and described in literature, we documented pervasively distributed young normal faults related to E-W extension at the kilometer-scale based on the analysis of satellite imagery and field work, and at the outcrop-scale between the southern Himalayan mountain front and the Indian-Chinese border. Additionally, we assessed normal faulting in fluviolacustrine sediments, including soft-sediment deformation. In the following sections, we use the term "macroscale" to describe faults traced over distances of hundreds of meters up to several kilometers, "mesoscale" for faults with several meters of fault zone observed in outcrops that can be traced over several meters, and "outcrop-scale" for faults and fault planes visible at a scale of a few centimeters up to a few meters.

Macroscale Normal Faults from Satellite Imagery and Field Observations

Area Southeast of Tso Morari

In addition to the 40-km-long Tso Morari normal fault (see Fig. 1B), there is a second en echelon set of parallel east-dipping normal faults to the southeast, which we term the eastern Tso Morari fault system (see Fig. 2). The two fault strands are exposed for 20 and 10 km, respectively, and are spaced ~2 km apart. In the central sector of the eastern fault, the fault diverges into a lozenge-shaped segment, which converges with the main fault ~5 km south. The eastern Tso Morari fault system separates sedimentary rocks of Neoproterozoic and Cambrian age and Ordovician granites in the footwall from fan gravels of inferred Quaternary age that constitute a large, contiguous bajada adjusted to the Pare Chu River. The alluvial fans in the hanging wall of the easternmost fault, as well as fluvial terraces parallel to the Pare Chu River, which crosses the fault, are apparently not displaced by the fault (Fig. 2).

Approximately 6 km east, the landscape is dissected by numerous W- to WNW-dipping normal faults (Fig. 2). The fault scarps are less pronounced compared to the eastern Tso Morari fault system, but they strike N-S. These faults clearly show evidence for top-to-the-west normal faulting. Similar to the larger, east-dipping faults on the west, the fluvial deposits of the Pare Chu River and its tributaries are not displaced by these west-dipping faults, and therefore they postdate faulting in this region (Fig. 2). However, the normal faults offset gently inclined erosion surfaces that were sculpted into the Proterozoic to Paleozoic basement rocks (see eastern part of Fig. 2). These surfaces are interpreted to represent a pediment surface that was formerly adjusted to a higher base level of the Pare Chu River, but that became subsequently abandoned due to base-level lowering.

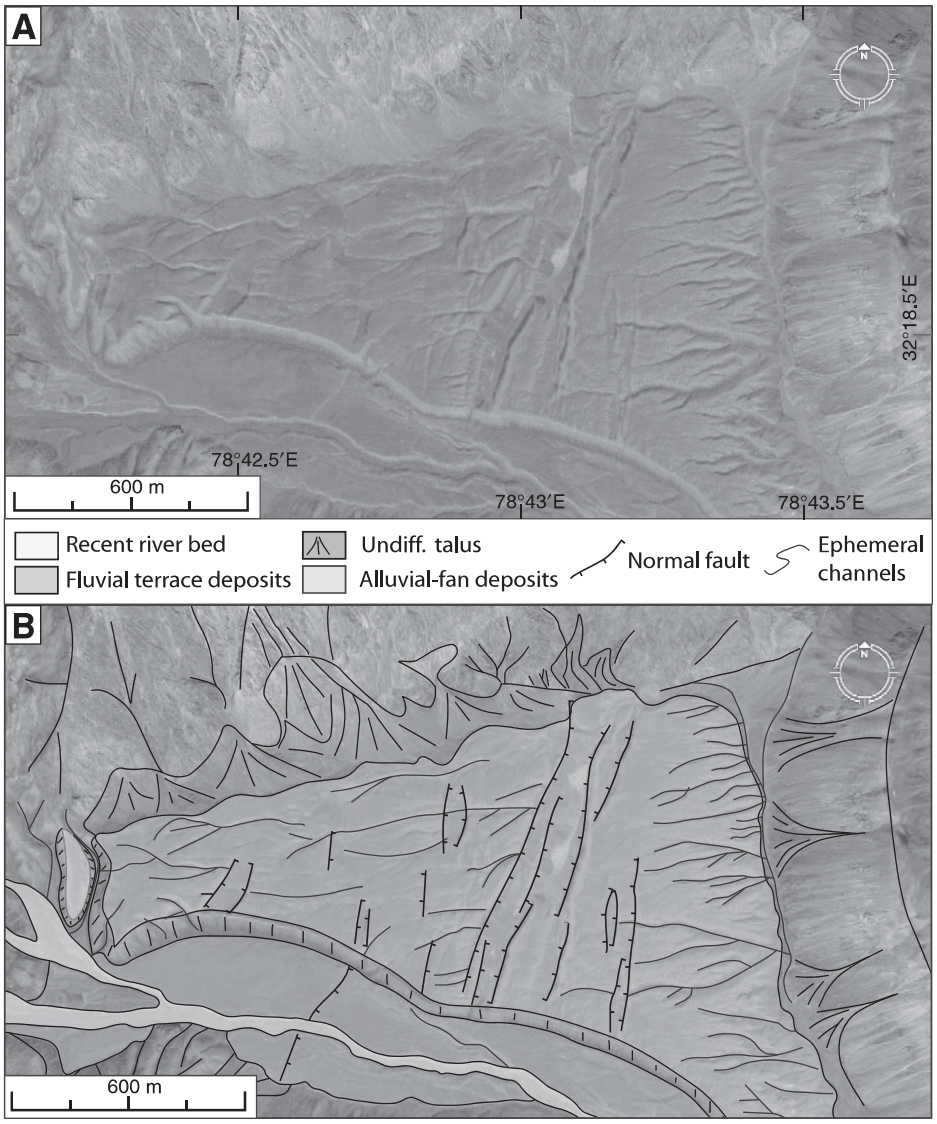

Figure 4. Normal faults of inferred Quaternary age in the NW Leo Pargil basin. E- and W-dipping faults displace an alluvial fan and a younger fluvial terrace (image source: GoogleEarth). Ephemeral channels are affected by normal faulting and were used to determine the dip direction of the normal faults. See Figure 1B for location.

Normal Faulting North of Leo Pargil

One of the most striking preserved young features affected by normal faulting is an extensive, originally contiguous gravel-covered paleosurface with ubiquitous erosional remnants in a formerly closed sedimentary basin northwest of the Leo Pargil gneiss dome (for location, see Fig. 1B). The basin is bounded by E- and W-dipping normal faults. In the center, the paleosurface consists of large, gently NE-tilted segments that are incised by small streams. The geomorphic character of the surface remnants and their lower eroded sectors is similar to features observed in the Zada Basin of the upper Sutlej River, southeast of the Leo Pargil gneiss dome. Based on similar outcrop and geomorphic characteristics, we infer that this surface constitutes the remnant of extensive gravel-covered lacustrine marls that once filled the basin before the current rivers started incising and eroding the basin fill due to headward erosion.

Based on the degree of preservation of the fault scarps, what we infer to be the oldest normal faults occur at the eastern and western margins of the basin. Movement along these structures created accommodation space for the sedimentary fill, which is now being incised and evacuated. Farther basinward toward the east, there are also morphologically younger N-S–striking faults that offset fluvial-terrace and alluvial-fan surfaces that have prograded into the basin fill in the course of down-cutting. These surfaces thus postdate the extensive basin fill and are located at a lower elevation than the top of the surface that forms the youngest part of the basin-fill unit. However, the youngest alluvial-fan deposits in this area cover the faults and clearly postdate tectonic activity along these older normal faults (Fig. 3).

The western margin of the basin is delimited by east-dipping normal faults, which are readily identified on satellite imagery. The normal faults constitute a sharp boundary between the basement rocks in the footwall and the sedimentary cover in the hanging wall. Several terrace levels in the northern part of the basin indicate that the

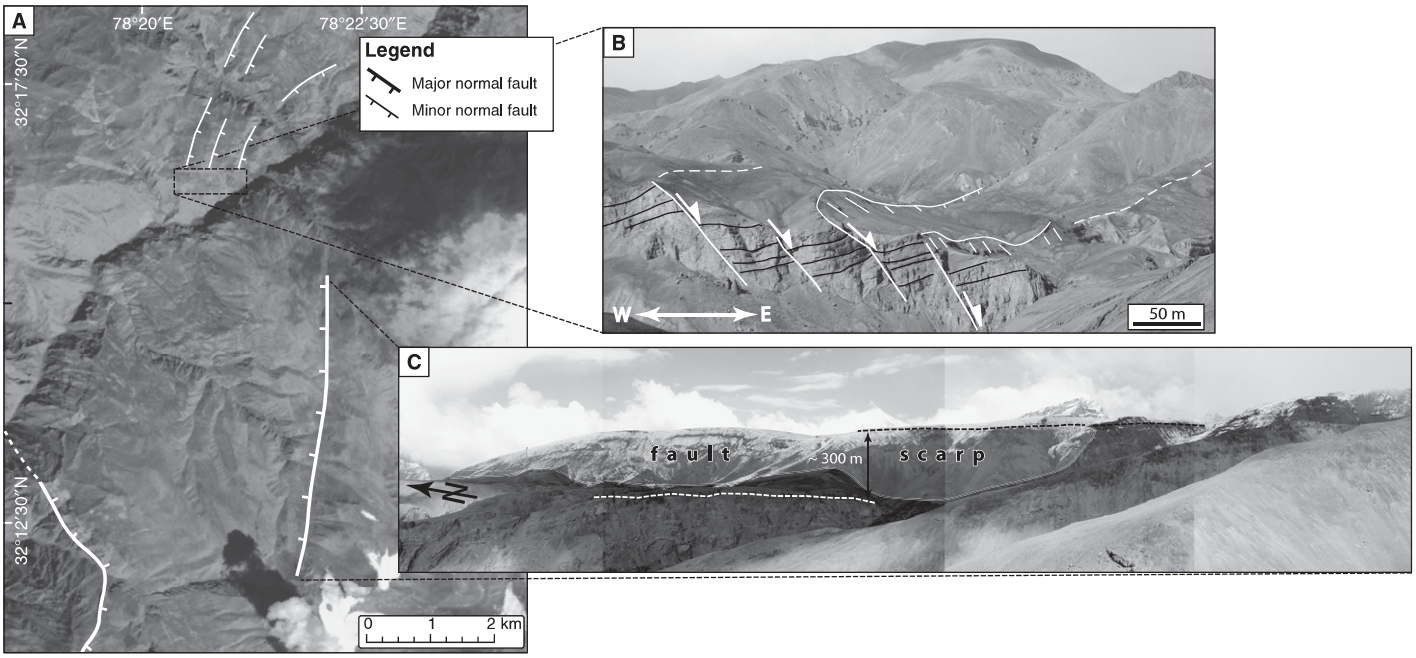

Figure 5. Normal faults in the Lingti Valley. (A) Overview of the Lingti Valley with normal faults and locations of panels B and C (image source: ASTER). (B) Normal faults dipping to the ENE arranged in bookshelf manner. A minimum vertical displacement on each fault strand of ~20 m can be inferred from correlating the layers across the fault planes. (C) Normal fault with a fault scarp dipping to the W; dotted line denotes ~300 m normal offset of gravel-covered erosion surface in Jurassic basement. See Figure A for location.

paleosurface was displaced by normal faulting. In contrast, multiple extensive terraces observed along most of the larger rivers in the southern part of the basin are not displaced and thus also postdate activity along the border faults.

More recent normal faulting affecting an alluvial fan of inferred Quaternary age and subrecent fluvial terrace deposits is observed within the basin center (see Fig. 4). This has resulted in a horst-and-graben morphology, which indicates that normal faulting is still active.

Lingti Valley

In the Lingti Valley, between the Tso Morari Lake in the north and the Spiti Valley in the south, prominent N-S–striking normal faults can be identified on satellite imagery (Fig. 5A). The most prominent normal fault is exposed east of the Lingti River and can be traced for ~8 km. Our field observations confirm that this fault dips to the west and has a vertical displacement of several hundred meters (Fig. 5C). An undated erosional paleosurface sculpted into Jurassic carbonates and preserved at an average elevation of 4700 m within the hanging wall is displaced by this fault and subsidiary structures. Furthermore, there are brittle normal faults arranged in bookshelf manner on the western border of the Lingti River that affect the same erosional paleosurface (Fig. 5B). These latter structures dip ENE. A minimum vertical displacement on each fault strand of ~20 m can be inferred from correlation of the layers across the fault planes (Fig. 5B). In the lower parts of the valley, steeply dipping brittle faults striking N-S are observed. Limited striations on these fault planes plunge downdip and, therefore, fit into an overall E-W extensional regime.

Our observations in this area are consistent with mapping of normal faults by Neumayer et al. (2004) at different length and displacement scales, ranging from mesoscale features to several-kilometer-long structures in the southernmost part of the valley. Similarly, these authors related the normal faults to E-W extension and interpreted them as representing the youngest tectonic movements in the region.

Mesoscale and Outcrop-Scale Faults Observed in the Field

Mesoscale and outcrop-scale brittle normal faults are ubiquitous in the area surrounding the Tso Morari–Leo Pargil seismic zone and document the extent of active normal faulting in the Higher Himalaya and also south of the Southern Tibetan detachment system (Fig. 6). Our field observations reveal a network of small-scale normal faults that cannot be detected on satellite imagery. Between the Spiti River in the north and the Main Boundary thrust in the south, numerous steeply dipping N-S–striking normal faults and extensional fracture zones form a dense network, with surface disruptions virtually every 15–20 m (Fig. 7A). Identical to the large-scale structures described previously, these faults result from E-W extension and crosscut all older structures. Taken together with all other sites visited in the field, these structures thus represent the most recent phase of deformation in this part of the Himalaya.

In addition, prominent N-S–striking normal faults with gouge zones up to 3 m wide dominate a diffuse band between 78°E and 78.5°E. They are typically associated with steeply plunging striations indicating dip-slip faulting and E-W extension. In most cases, smaller, parallel, brittle fault planes are observed in their vicinity. Because none of these faults is overprinted by any other structure, we infer that they also reflect the youngest phase of deformation in the region. Synkinematic micas on fault planes and within fault gouges indicate that these faults were associated with deeper-seated processes and originated in the brittle-ductile transition zone but have been exhumed since. Consequently, the faulted basement rocks exposed at the surface today were initially deformed by E-W extension at greater depths, suggesting that this style of deformation has been sustained over long time scales. In the exhumed orthogneisses of the footwall of the southernmost sector of the Leo Pargil detachment zone, we found synkinematically grown

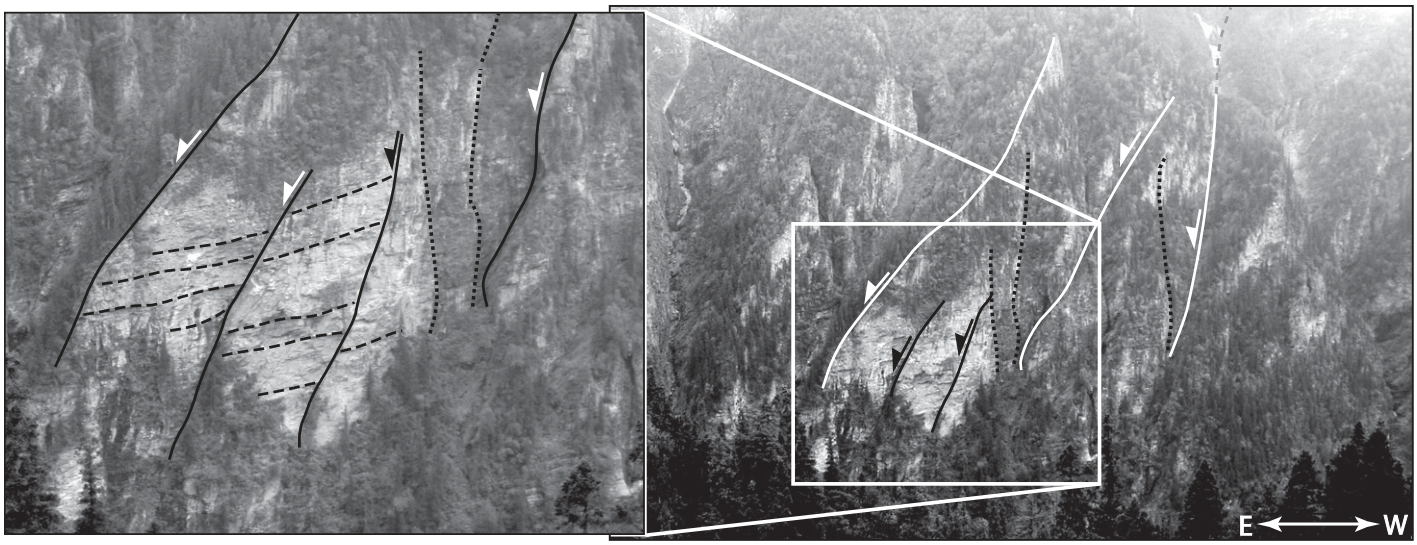

Figure 6. Approximately E-dipping brittle normal faults in the granitic gneisses of the Higher Himalaya close to the Main Central thrust in the Parbar Valley (Garhwal Himalaya). Left panel shows a close-up of the area marked with a white box in the right panel. Solid lines mark the fault traces; dashed lines show foliation orientation. Dotted lines mark the orientation of possible Riedel-shear planes. Note trees in the front for scale. See Figure 1B for location.

muscovites on a west-dipping fault (strike/dip 178/83°W; see marked location in Fig. 7B) associated with a steeply dipping lineation (trend/plunge: 280/82°W). The $^{40}Ar/^{39}Ar$ dating of these micas provides ages of 16.3 ± 0.04 Ma and 16.9 ± 0.04 Ma (see Table 1; Fig. 8). This age coincides with the onset of exhumation of the Leo Pargil gneiss dome at 16–14 Ma, also derived from $^{40}Ar/^{39}Ar$ mica cooling ages farther north (Thiede et al., 2006). Therefore, it is possible that normal faulting in the hanging wall of the Leo Pargil detachment zone had already started before this time. However, the $^{40}Ar/^{39}Ar$ age presented here can be considered as a lower boundary for the onset of E-W extension in the NW Indian Himalaya.

Normal Faults in Sediments and Soft-Sediment Deformation

With the exception of the spatially limited Quaternary basin fills described previously herein, mostly Paleozoic basement rocks are affected by normal faults in the Higher and Tethyan Himalaya due to the virtual absence of Cenozoic deposits at these high elevations. Hence, it is difficult to unambiguously constrain onset and duration of extensional processes in this region. In places, weathered conglomeratic gravel of unknown age overlying basement rocks is affected by extensional fractures and normal faults. In particular, at the junction of the Spiti River and its tributary, the Lingti River, ~2 m of fine-grained, gray, alluvial-fan sediments are overlain by 1.5 m of laminated sandy-silty lake sediments (Fig. 9). Both units are displaced by several N-S–striking normal faults. A slightly older generation of NW-SE–striking normal faults is systematically displaced by the N-S–striking faults, supporting our inference that N-S–striking normal faulting reflects the youngest phase of deformation in the NW Indian Himalaya. However, because the NW-SE–striking normal faults are approximately parallel to the trend of the regional slope, it may be possible that this fault set is not tectonic in origin but instead results from gravity sliding. In contrast, the N-S–striking faults are oblique to the regional slope; a gravitational origin can thus be excluded. Interestingly, some fault planes end in layers that have flame structures, typically associated with deformation during earthquakes (Fig. 9). This observation suggests a possible seismogenic origin of these faults. OSL dating of these deposits provides a burial age of 39.9 ± 2.2 ka for the interface between the alluvial-fan sediments and the lake sediments, illustrating the recent nature of seismogenic processes in the Tethyan Himalaya, which is in line with the instrumentally recorded seismicity in this region (e.g., Molnar and Chen, 1983).

Evidence for soft-sediment deformation of lacustrine sediments is also observed farther east, along the lower Spiti River near the western flanks of the Leo Pargil gneiss dome, where lake deposits reach a thickness of up to 100 m. They extend along the valley for ~8 km and are located between 10 and 100 m above the recent river bed (Fig. 10). The sediments are mainly composed of clay with intercalated thin sandy or silt layers, which are between 0.5 and 10 cm thick. In several locations within the lacustrine sediments, we identified soft-sediment deformation phenomena, such as flame structures, neptunic dikes, and intruded lenses of conglomerates (Fig. 10). All these phenomena can be traced laterally up to 50 m. OSL dating of the sandy layers above the strata affected by soft-sediment deformation provides ages of 29.2 ± 1.6 ka at point B and 31.7 ± 3.9 ka at point D, indicating that the sedimentary deposits at those outcrops are related to the same lake. The OSL ages at points A and C are given as 5.61 ± 0.48 ka and 21.3 ± 1.1 ka, respectively, showing that there are several generations of lake deposits in this region. Details of the OSL dating results are given in Table 2.

Interestingly, soft-sediment deformation within different lacustrine sedimentary bodies is found mainly in the vicinity of the Kaurik-Chango normal fault. Given the proximity to the regional active tectonic structures, the soft-sediment deformational structures could be seismogenic. The last large earthquake on this fault (Kinnaur earthquake, 19 January 1975, M = 6.5, fault-plane solution labeled with KEQ in Fig. 1B) produced surface ruptures on the order of 0.5 m (Singh et al., 1975; Bhargava et al., 1978). Due to the absence of a present-day lake in the source area of the 1975 Kinnaur earthquake, a comparison between recently produced seismogenic features and our inferred older, possibly earthquake-induced soft-sediment deformation

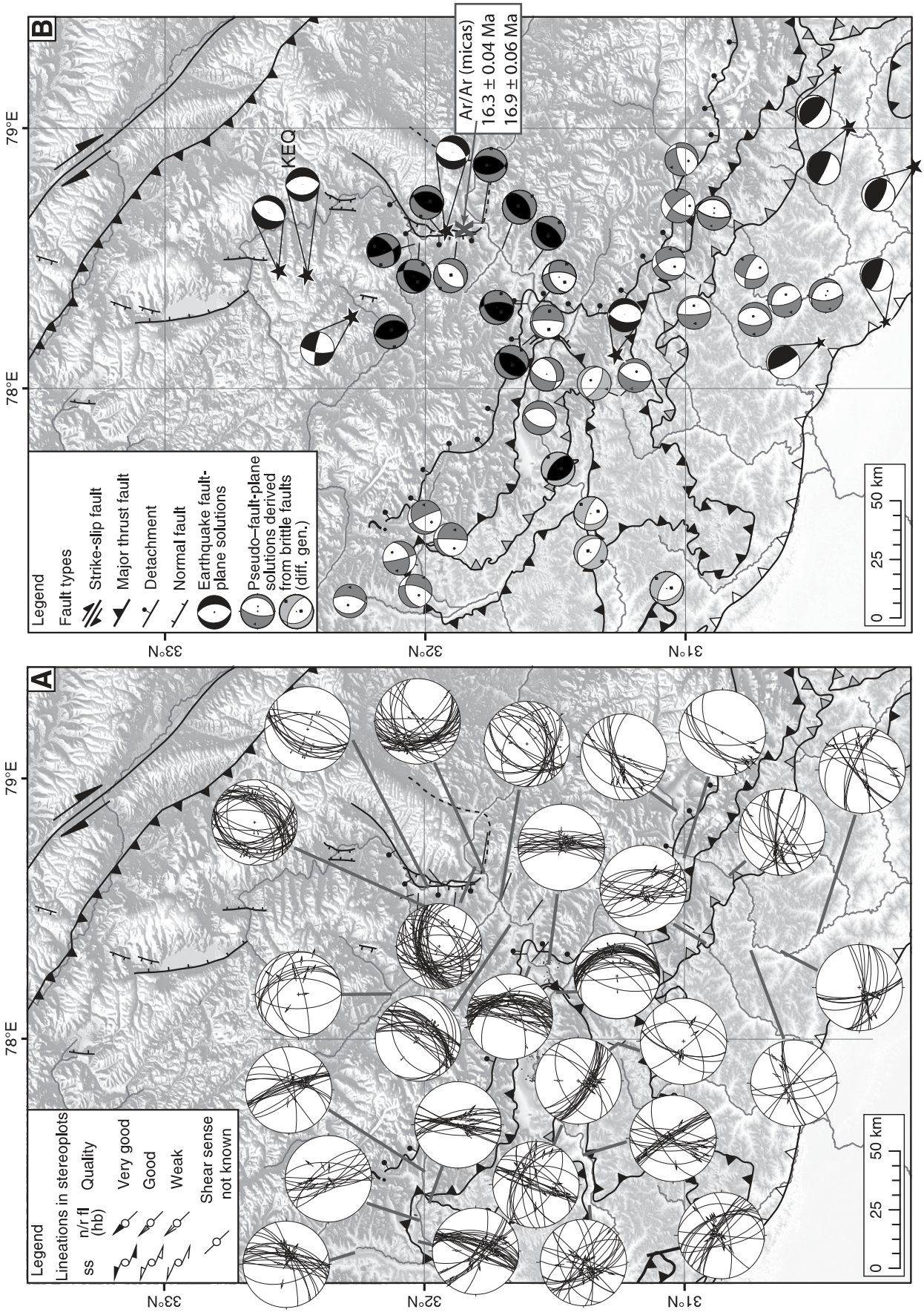

Figure 7. (A) Combined kinematic information of brittle deformation (fault planes and striations) in the NW Indian Himalaya. Data close to the Leo Pargil dome were previously published by Thiede et al. (2006). (B) Synopsis of the pseudo–fault-plane solutions shown in different gray colors based on the data shown in A. For details for obtaining the pseudo–fault-plane solutions, see text. For details about the $^{40}Ar/^{39}Ar$ ages, see text, Table 1, and DR1 (GSA Data Repository [see text footnote 1]). Structural map and base map showing elevation are the same as in Figure 1B.

TABLE 1. SUMMARY OF $^{40}AR/^{39}AR$ DATA
(AGE UNCERTAINTIES INCLUDE ERROR IN IRRADIATION PARAMETER *J*)

Sample	Weight (mg)	TFA (Ma)	WMPA (Ma, ±2σ)	IA (Ma, ±2σ)	Steps used (total steps)	% ^{39}Ar
B270901-3	3.2	16.4	16.3 ± 0.04	16.3 ± 0.04	8–23 (23)	87
B270902-4	3.3	17	16.9 ± 0.06	16.9 ± 0.14	8–16 (21)	39

Note: TFA—total fusion age; WMPA—weighted mean plateau age; IA—isochron age. Detailed information is available in GSA Data Repository DR1 (see text footnote 1).

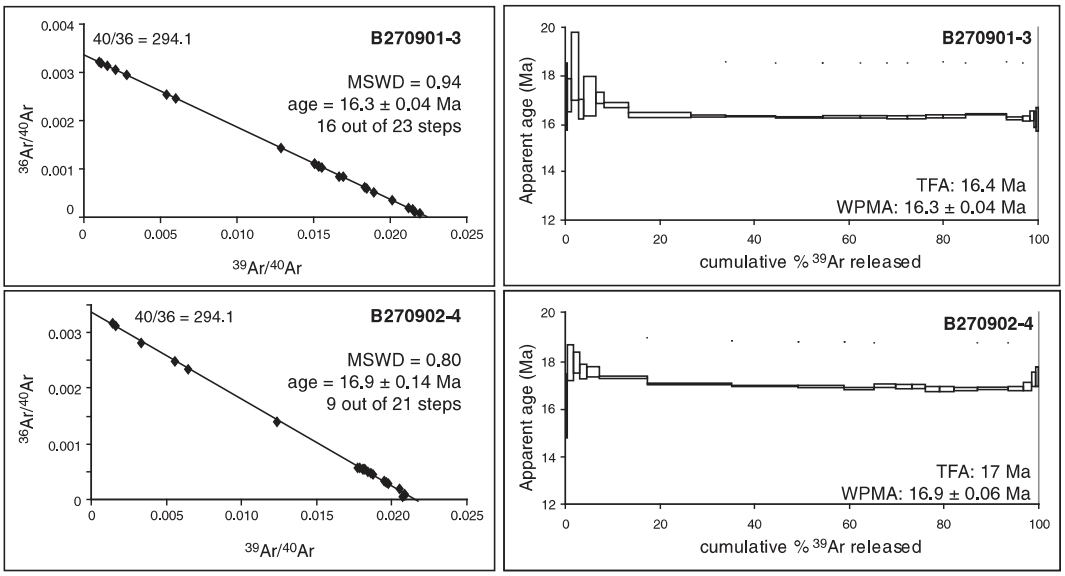

Figure 8. $^{40}Ar/^{39}Ar$ ages in inverse isochron and spectra diagrams measured on white mica from rocks within the footwall of the Leo Pargil detachment zone. Increments indicate number of temperature steps considered for the age termination with the isochron plot. Both samples yield well-constrained plateau ages of 16.3 and 16.9 Ma. TFA—total fusion age; WMPA—weighted mean plateau age; MSWD—mean square of weighted deviation.

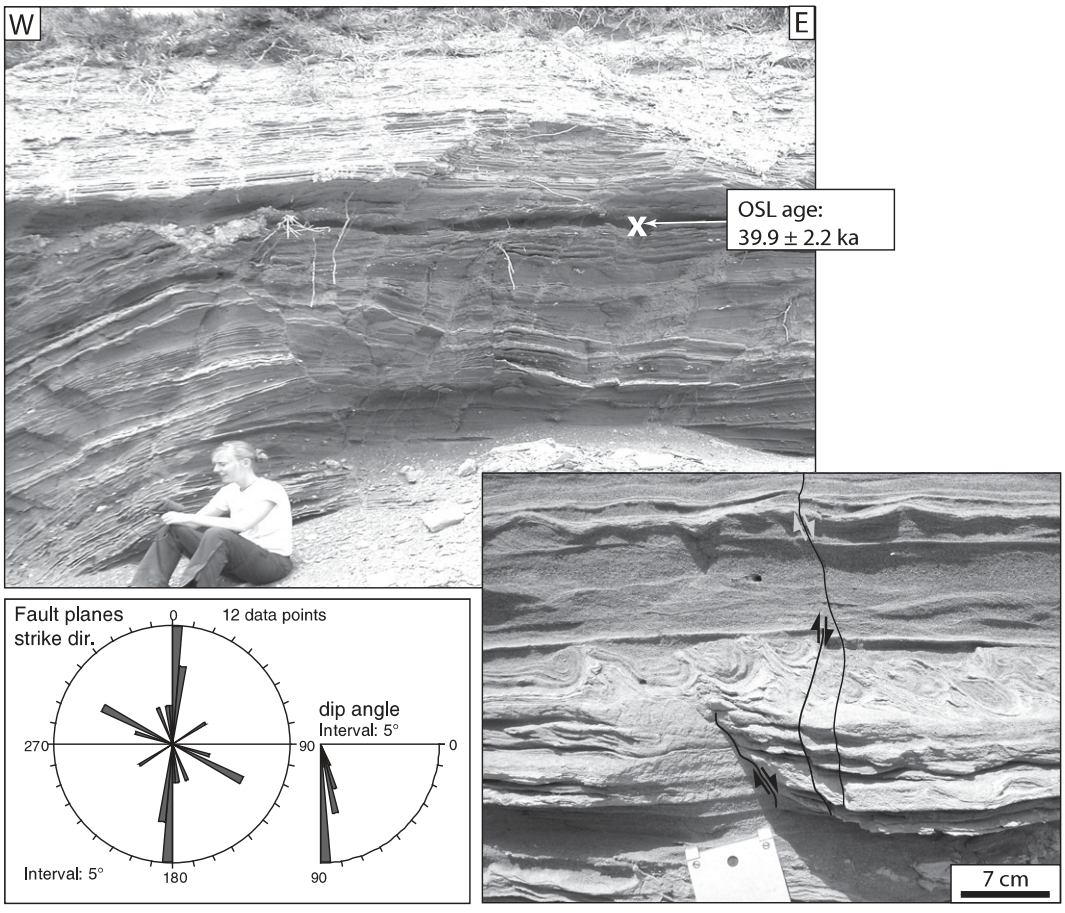

Figure 9. Fluvio-lacustrine sediments in the upper Spiti Valley, at the junction to the Lingti Valley. The sediments are affected by normal faulting. The two fault populations strike N-S and 105–285. Some of them terminate in layers with soft-sediment deformation typically associated with deformation during earthquakes (lower-right inset). See Figure 1B for location

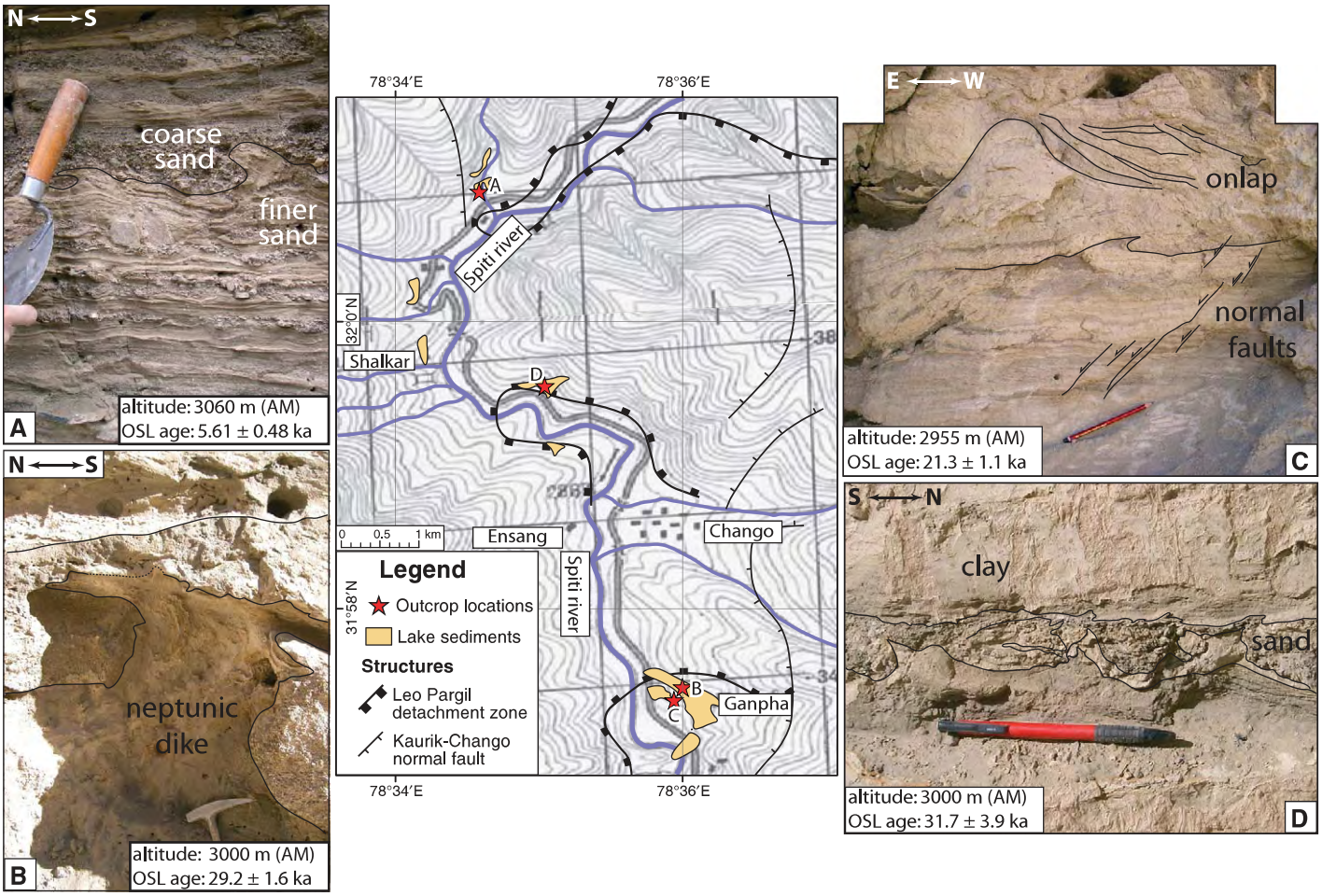

Figure 10. Lake sediments in the lower Spiti Valley affected by soft-sediment deformation (A–D). Thin black lines delimit layers of fine sandy layers, coarse sandy layers, and/or clay layers. Locations of field photos are marked in center (A–D). Geological information was taken from Thiede et al. (2006).

TABLE 2. OPTICALLY STIMULATED LUMINESCENCE (OSL) DATING RESULTS

	Location			Dose rate analysis					OSL dating results			
Sample	Latitude (°N)	Longitude (°E)	Depth (m)	U (ppm)	Th (ppm)	Rb (ppm)	K (%)	Moisture (%)	Aliquots meas. (used)	Paleodose (Gy)	Dose rate (μGy/yr⁻¹)	Age (ka)
Point A	32.0151	78.5764	3	1.6	7.0	43.1	0.66	0.3 ± 5	14 (11)	9.9 ± 0.7	1756 ± 79	5.61 ± 0.48
Point B	31.9575	78.6001	50	4.57	17.9	112	1.57	0.3 ± 5	13 (9)	120 ± 3.1	4103 ± 202	29.2 ± 1.6
Point C	31.9560	78.5990	2	3.15	12.9	102	1.44	0.6 ± 5	16 (14)	73 ± 1.6	3414 ± 159	21.3 ± 1.1
Point D	31.9925	78.5840	75	3.9	16.1	88.5	1.34	0.6 ± 5	3 (1)	113 ± 13	3576 ± 170	31.7 ± 3.9
Lingti	32.1088	78.1829	1.5	4.46	21.7	103	1.50	0.4 ± 5	12 (12)	180 ± 5.6	1221 ± 64	39.9 ± 2.2

Note: Location of samples: sample name refers to map points in Figure 10, "Lingti" is related to the contact of alluvial-fan and lacustrine deposits in Figure 9. Dose rate analysis: Content of naturally occurring potassium (K), thorium (Th), rubidium (Rb), and uranium (U) within the sample material, which are the main contributors of dose to sedimentary quartz. OSL dating results: total dose rate is attenuated for grain size, density, and moisture.

features is not possible. However, although other mechanisms could be invoked locally, the close relationship between normal faults and various types of soft-sediment deformation features in lake sediments in the immediate vicinity of the seismically active belt between the Tso Morari Lake and the Leo Pargil gneiss dome suggests a cogenetic origin.

PALEOSTRAIN RESULTS

We collected fault kinematic information at ~100 outcrops between the Tso Morari dome in the north and the Lesser Himalaya in the south. We focused on the southern continuation of the Tso Morari–Leo Pargil seismicity zone and the area between the Leo Pargil gneiss dome in the east and the Kullu Valley in the west. We only considered brittle faults that could be clearly assigned to the youngest deformation phase in the area. The striations on the mainly N-S–striking normal faults related to this deformation phase are typically steeply dipping. However, there are several instances where older fault planes have been reactivated

as oblique normal faults. In total, we selected ~30 outcrops where we had sufficient data related to the youngest deformation phase in the local context. For these measurements, we calculated pseudo–fault-plane solutions (Fig. 7B).

The majority of the pseudo–fault-plane solutions shows chiefly E-W extension. In the vicinity of the Leo Pargil gneiss dome, the extension direction is NW-SE. In the southwest of the study area, the extension direction is NE-SW, and thus perpendicular to the strike of the orogen (light-gray pseudo–fault-plane solutions in Fig. 7B). Clear crosscutting relationships between fault planes associated with these different extension directions are rare. Observations at a single outcrop indicate that fault planes related to the NE-SW extension have been locally overprinted by faulting during E-W extension.

Diffuse E-W–oriented extension is observed in virtually the entire study area. However, the density of fault planes dipping steeply W or E in the region associated with the N-S seismicity belt is much greater, and enhanced seismicity between the Tso Morari Lake and the Leo Pargil gneiss dome is much more pronounced compared to other regions of the study area. Nevertheless, at present, we have no data to test if this zone of focused seismicity is a temporary, short-lived feature, or if it is important over longer geologic time scales.

DISCUSSION AND CONCLUSIONS

The new data we present here, including map-scale normal faults identified on satellite imagery and in the field, mesoscale faults, outcrop-scale fault-kinematic data, and fault-cut Quaternary sediments, document ongoing normal faulting extending from the Greater Sutlej River region to the Garhwal Himalaya. The different observations record E-W–oriented extension over a diffuse, approximately N-S–striking swath between 77.5°E and 79°E. Next, we first address the possible onset and/or ages of the different evidences for deformation, and secondly discuss their origin and possible underlying driving mechanisms.

Possible Onset of E-W Extension in the Higher Himalaya

A comparison of our own newly derived $^{40}Ar/^{39}Ar$ and OSL ages with already published studies in the NW Himalaya allows us to estimate the possible ages of the onset of normal faulting and its continuation to the present day. The following sections discuss the possible timing for the different types of extensional features, where available.

Brittle Faulting on Mesoscale and Outcrop Scale

Synkinematic micas on fault planes and within fault gouge and quartz-filled tension gashes suggest that at least part of the brittle faulting related to E-W extension has its origin in the brittle-ductile transition zone. This zone broadly coincides with depths where temperatures are around 350 °C. The $^{40}Ar/^{39}Ar$ cooling ages of micas recording a closure temperature of ~350 °C have age ranges between 14 and 19 Ma for the Higher Himalaya, and 4.3–6.7 Ma for the Lesser Himalayan crystalline sequence between the Munsiari thrust and Main Central thrust, respectively (Vannay et al., 2004; Thiede et al., 2005, 2006). These ages can be thus considered as the older limit of brittle-deformation behavior of the rocks. The age obtained for synkinematic muscovites on a fault plane in the footwall of the Leo Pargil gneiss dome in our study provides a similar age constraint of ca. 16 Ma (see Figs. 7 and 8). Because those micas are synkinematically grown on a fault that is compatible with the E-W tension, we infer that E-W extension was already active in the Higher and Tethyan Himalayas at that time. In addition, ductile mineral stretching lineations observed in the footwall of the Leo Pargil detachment zone along the western flank of the Leo Pargil also indicate E-W extension at lower structural levels between 14 and 16 Ma (Thiede et al., 2006). Combining all of these observations, we suggest that E-W extension was initiated at least around 4 Ma in the Lesser Himalaya and between 14 and 16 Ma in the Higher and Tethyan Himalayas.

Large-Scale Normal Faults on Satellite Imagery

Age constraints on the large-scale normal faults that we evaluated mainly from satellite imagery are essentially nonexistent. The age of the faulted paleosurface in the Tso Morari area and in the Lingti Valley is unknown, but based on regional relationships, it can be estimated with reasonable certainty to be of Quaternary age.

In the sedimentary basin NW of the Leo Pargil gneiss dome, however, a rough age estimate can be made. The sedimentary fill is clearly related to transient basin isolation, and we infer that normal faulting caused hydrologic isolation and the generation of accommodation space for sediments. The onset of basin filling, therefore, must have been simultaneous with the beginning of normal faulting, and the partially preserved paleosurface provides a minimum timing for the onset of normal faulting in this basin.

Despite a lack of radiometric ages to further decipher these processes, the age of the sedimentary basin fill may be comparable to the fill units of the much larger Zada Basin on the SE side of the Leo Pargil dome, and a crude age estimate may be possible based on observations there. Saylor et al. (2009) suggested that the oldest sedimentary deposits in the Zada Basin are late Miocene. Normal faults along the eastern flank of the Leo Pargil gneiss dome constitute the western border of this basin. Hence, if these normal faults are mechanically linked and are an integral part of the extensional structures that characterize this dome, the structures on the western flank of the dome and the sedimentary fills are coeval.

Soft-Sediment Deformation

Soft-sediment deformation features along the western flank of the Leo Pargil gneiss dome occur in lacustrine sediments that were deposited in a landslide-dammed lake (Bookhagen et al., 2005). The ^{14}C ages of the lowest part of these sediments show a consistent calibrated age of 28.5 ± 0.9 ka (Bookhagen et al., 2005). Our OSL ages of sandy layers immediately above those strata affected by soft-sediment deformation provide similar ages within error, attesting to the recent nature of seismogenic movements in this region and to protracted activity along the Kaurik-Chango normal fault. Mohindra and Bagati (1996) and Banerjee et al. (1997) reported similar features in the Pare Chu Valley directly north of the area shown in Figure 10. Based on OSL dating and sedimentary analysis, these authors inferred at least nine separate earthquakes with magnitudes large enough to produce soft-sediment deformation within the last 90 k.y. Because the soft-sediment deformation features that we observed are only a few kilometers away from these lacustrine sediments, they all likely underwent soft-sediment deformation in the same tectonic environment. Thus, there is widespread evidence for seismic activity along the Kaurik-Chango normal fault indicating E-W extension since at least the Pleistocene.

Possible Mechanisms for E-W Extension in the Tethyan and Higher Himalaya

Models and interpretations of orogen-perpendicular grabens in the Central Himalaya can be separated into three major groups: (1) models linking the graben systems to escape tectonics in the course of the India-Eurasia collision process (e.g., Tapponnier and Molnar, 1976; Tapponnier et al., 1982); (2) models that relate the arc-perpendicular structures to the arcuate geometry of the Himalaya and/or the Indian subduction zone (e.g., Ratschbacher et al., 1994); and (3) models invoking processes such as slip partitioning resulting from oblique convergence

(McCaffrey and Nabelek, 1998) or local extension due to metamorphic dome formation (e.g., Aoya et al., 2005). In Table 3, we summarize the major hypotheses as well as their implications for extensional structures in the NW Himalaya and consider if they are applicable to our region.

Models explaining arc-parallel extension in the Central Himalaya based on the arcuate shape of the orogen predict normal faults that are generally perpendicular to the regional trend of the Himalaya. Due to the regional NW-SE trend of the NW Indian Himalaya, these models would predict a NW-SE–oriented extension direction. This is inconsistent with our field observations, as well as the results of our brittle-fault kinematic analysis, which show E-W–directed extension. Furthermore, it is incompatible with the kinematic character derived from regional GPS measurements (Banerjee and Bürgmann, 2002) and extension directions obtained from focal mechanisms of larger earthquakes in the NW Indian Higher and Tethyan Himalaya (Molnar and Chen, 1983; Molnar and Lyon-Caen, 1989). These inconsistencies require alternative mechanisms to explain the observed E-W extension. Next, we assess three possible scenarios that could explain ongoing extension processes in this part of the mountain range.

The first, and rather local, explanation for the existence of brittle normal faults is their potential association with the Leo Pargil gneiss dome immediately east of our study area (see Fig. 1B). Similar to other active gneiss domes in the western Himalaya, it is associated with extensional structures at its flanks (Murphy et al., 2002; Thiede et al., 2006; Saylor et al., 2009). The presence of normal faults in the vicinity of the gneiss dome would be related to accommodation of different exhumation rates between the buoyant gneiss dome and the surrounding region.

A second possible explanation for the normal faults involves a horsetail termination of the neighboring dextral Karakorum fault (Figs. 1A and 11A). The eastward escape of central and northern Tibet is mainly accommodated along regional sinistral and dextral strike-slip faults at the northern and southern plateau margins, respectively (e.g., Peltzer and Tapponnier, 1988; Taylor et al., 2003). The southwestern margin of Tibet is bounded by the NW-SE–striking Karakorum strike-slip fault system, which can be traced 1000 km from the Pamir in the northwest to the Gurla Mandhata dome in the southeast (Fig. 1A; Murphy et al., 2000). Close to this gneiss dome, the low-angle, west-dipping Gurla Mandhata detachment zone is exposed. Geological field observations and $^{40}Ar/^{39}Ar$ chronology suggest a kinematic linkage of both faults (Murphy et al., 2002; Murphy and Burgess, 2006). If related, normal faults in

TABLE 3. MODELS FOR E-W EXTENSION IN THE TIBETAN PLATEAU (TP) AND THE HIMALAYA, THEIR IMPLICATIONS, AND SPECIFICATIONS FOR E-W EXTENSION IN THE NW INDIAN HIMALAYA AND FOR THE KARAKORUM FAULT (KF)

Model:	Observations from the NW Indian Himalaya:	E-W extension oblique to the regional trend of the orogen	Extent of E-W extension	E-W extension not limited to larger structures	Role of the KF	Normal faulting south of the South Tibetan Detachment System	Migration of extensional structures from the TP into the Himalaya
Local explanations	(1) Local extension due to dome formation of the Leo Pargil dome (e.g., Aoya et al., 2005)	Yes	Limited to the vicinity of the Leo Pargil gneiss dome	No, mainly focused to dome structures	Not predicted	Not predicted	No
	(2) Horse-tail termination of the KF (adapted after Kim et al., 2004)	Yes	SE of the KF	No, normal faults should be arranged in single splays originating at the KF	Large slip rate, greater impact	Not specified, but possible	No
Tibetan Extensional Models	(3) Oblique convergence between India and Asia (e.g., McCaffrey and Nabelek, 1998)	No	Southern Tibet and Himalaya above the subducting plate	No, slip is mainly concentrated on KF	Large slip rate, taking up all shear	Not specified, but possible	No
	(4) Change of boundary conditions along the eastern margin of Asia (Yin, 2000; Yin and Harrison, 2000)	Yes	Whole Asia, including the Tibetan Plateau (TP) and Himalaya	Yes	Not specified	Not specified, but possible	Yes
	(5) Gravitational collapse of the TP including continuous deformation and coupled crust and mantle (e.g., Zhang et al., 2004)	Yes	Entire TP and Himalaya	Yes	Not a major feature	Not specified, but possible	Yes
	(6) Extrusion of the TP along large strike-slip faults; no mantle flow involved; Tibet behaves as rigid blocks (e.g., Tapponnier et al., 1982)	Yes	Entire TP and Himalaya	Yes	Large slip rate, major feature	Not specified, but not likely	Yes
	(7) Convective removal of the lower mantle lithosphere (England and Houseman, 1989)	Yes	Entire TP and Himalaya	Yes	Not a major feature	Not specified	Yes
	(8) Gravitational collapse of the TP including decoupled crust and mantle by a weak lower crust (e.g., Nelson et al., 1996)	Yes	Entire TP and Himalaya	Yes	Not a major feature	Not specified, but not likely	Possible

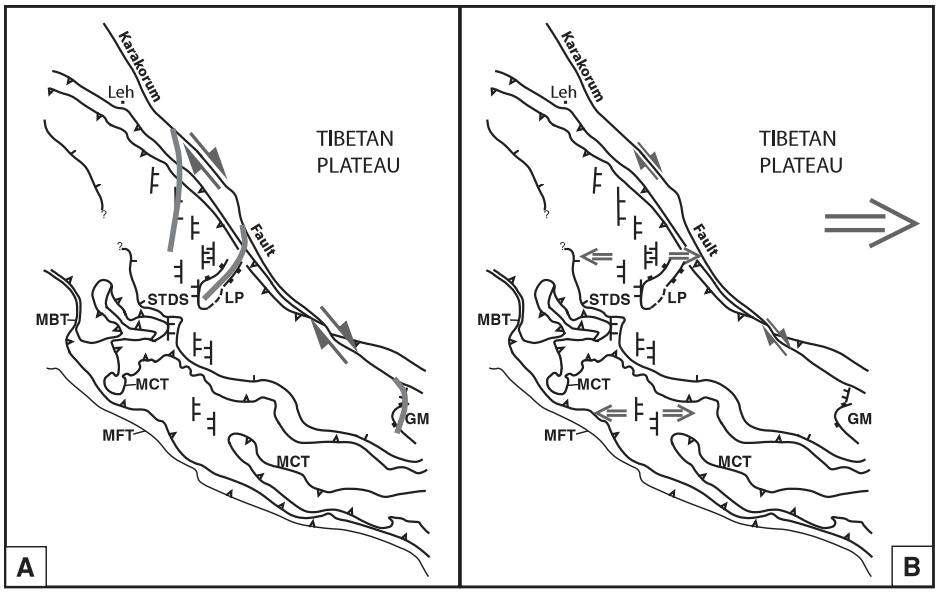

Figure 11. Schematic sketch of models for E-W extension observed in the NW Indian Himalaya west of the Karakorum fault (not to scale). (A) Horse-tail termination of the Karakorum fault. Gray lines show the inferred trend of the splays. Normal faults do not fit into this arrangement. (B) Transition of normal faulting from the Tibetan Plateau into the Himalayan realm. Arrows show the approximate extension direction observed in the Tibetan Plateau and in the NW Himalaya, as well as movement along the Karakorum fault. Major geological structures are from DiPietro and Pogue (2004). In the Higher and Lesser Himalaya, normal-fault symbols represent pervasive, closely spaced outcrop-scale normal faults. For abbreviations, see caption to Figure 1.

the greater Sutlej region could be an integral part of such a horsetail termination of this large strike-slip fault system (see Kim et al., 2004; Fig. 11A). Accordingly, the areas of localized normal faulting between the Tso Morari dome in the north and the Zada Basin in the south could be interpreted as single branches of a horsetail structure.

The third and final alternative explanation links normal faulting in the NW Indian Himalaya to southward propagation of active extensional processes on the Tibetan Plateau (Fig. 11B). For example, fault-plane solutions of earthquakes in this region show dominant E-W extension (Molnar and Chen, 1983; Molnar and Lyon-Caen, 1989). If the observed E-W extension in the NW Indian Himalaya is related to extension in the plateau, then the role of the Karakorum fault as a first-order boundary between the tensional stress regime in the Tibetan Plateau and compression in the Himalaya would be of secondary importance. The ongoing controversy concerning the displacement rate of the Karakorum fault (e.g., Lacassin et al., 2004; Chevalier et al., 2005; Searle and Phillips, 2007) underscores its ambiguous role in the recent deformation history of the Himalaya-Tibet region. If displacement rates are low (e.g., Searle et al., 1998; Murphy et al., 2000; Phillips et al., 2004) normal faulting in the Greater Sutlej region could indicate that the Karakorum fault has not been able to fully accommodate the E-W extension generated in the Tibetan Plateau. In this scenario, the Karakorum fault does not decouple the extensional processes in Tibet from the shortening regime in the Himalaya. Thus, extensional features in the NW Indian Himalaya would be linked to southward propagation of normal faulting and graben formation that is currently observed in Tibet and the transition with the Central Himalaya.

Whereas the first hypothesis has only local significance relevant for the immediate surroundings of the Leo Pargil gneiss dome, the other two hypotheses could explain normal faulting affecting much more extensive regions. Both hypotheses represent regional-scale end-member scenarios. One of the crucial issues in correctly assessing the different factors producing normal faulting is the importance of the Karakorum fault for recent deformation processes in the NW Himalaya. If the observed structures are indeed part of a horsetail termination of the Karakorum fault, this structure would represent a first-order decoupling zone between the Tibetan Plateau and the Himalaya. Conversely, if normal faulting were related to the propagation of extensional faulting originating on the Tibetan Plateau, then the Karakorum fault would be of secondary importance.

The three scenarios presented here may not be mutually exclusive. All present viable explanations for ongoing E-W–oriented extension in the Higher Himalaya of NW India. However, the overall distribution and orientation of normal faults is inconsistent with the hypothesis of doming and tectonic exhumation of the Leo Pargil gneiss dome. If doming were the primary driver for extension, normal faults should be concentrated close to the flanks of the gneiss dome and not in a N-S–striking swath of active faulting and seismicity that affects all preexisting contractional structures. Furthermore, the normal faults should be oriented radially around the outline of the gneiss dome; however, this is not the case. The processes responsible for doming at the Leo Pargil gneiss dome may still contribute to the evolution of local normal faults. In particular, the rotation of the extensional axis from E-W to NW-SE in the vicinity of the gneiss dome could be a result of doming. Nonetheless, doming does not appear to be a viable mechanism to explain the regional extent of E-W extension observed in the NW Indian Himalaya.

The two remaining end-member models that involve the Karakorum fault may better reconcile the observed structural evolution of the NW Indian Himalaya. In the model that relates the observed E-W extension with the horsetail termination of the Karakorum fault, single splays of normal faults perpendicular and south of this major structure would be expected. Our observations, however, did not reveal such single splays. Furthermore, the strike of such splay faults should rotate toward the Karakorum fault into a NW-SE direction, i.e., parallel to the strike of the Karakorum fault, as indicated by the gray lines in Figure 11A. This should be particularly true for smaller-scale structures. This is not the case, as was clearly shown by Epard and Steck (2008), who mapped Quaternary normal faults in the area between the Tso Morari and the Karakorum fault, immediately north of our study area. These faults do not show any change in strike direction close to the Karakorum fault. In addition, if there were a kinematic linkage between the long-lived Karakorum fault and E-W extension described here, the normal faults should have accrued higher total strain. This would imply that such faults would be more or at least equally pronounced as those normal faults observed around the Gurla Mandhata dome at the southernmost end of the Karakorum fault and south of our study area (Murphy et al.,

2002). Even if we cannot provide the exact amount of total normal displacement in the area, it is most likely less than the 35–66 km slip observed at the Gurla Mandhata dome (Murphy et al., 2002). This indicates that the mechanistic linkage between the N-S–striking normal faults in the NW Indian Himalaya and the Karakorum fault is not likely. Therefore, we also discard this hypothesis as an explanation for E-W extension in the NW Indian Himalaya.

The second end-member model predicts that E-W extension is transferred from the Tibetan Plateau into the NW Himalaya. In this scenario, the Karakorum fault would be a second-order feature. If the Karakorum fault indeed accommodated all of the E-W extension observed in the Tibetan Plateau, the level of seismic activity should be much higher than the present-day level of activity. Globally recorded seismicity in this area shows that only a few earthquakes have occurred along this fault in the past 30 years (NEIC Catalog). We thus infer that the Karakorum fault does not fully accommodate the bulk of E-W extension occurring in the Tibetan Plateau, and, therefore, part of this strain must be transferred SW of the Karakorum fault into the NW Indian Himalaya. This hypothesis explains why E-W extension in the NW Indian Himalaya is a pervasive, ubiquitous phenomenon independent of local structures. The N-S–striking normal faults would thus be an integral part of the same extensional processes that dominate the Tibetan Plateau and the transition to the Central Himalaya.

Among those models explaining E-W extention in the Tibetian Plateau, there are two main differences: (1) models that assume the crust and mantle are decoupled, with eastward extrusion of Tibet either accommodated as a rigid block bounded by large fault systems such as the Karakorum and Altyn Tagh faults (e.g., Tapponnier et al., 1982) or through continuous deformation distributed over the whole area (Taylor et al., 2003; Zhang et al., 2004); and (2) models that assume the upper brittle crust is coupled to the mantle (e.g., Molnar and Chen, 1983) or there is a weak lower-crustal level that decouples the mantle from the upper crust (e.g., Nelson et al., 1996). Our data suggest that the transition of extensional tectonics from the Tibetan Plateau across the Karakorum fault into the NW Himalaya may be related to a crust coupled to eastward-flowing mantle and continuous deformation not restricted to single larger structures. With the data presented here, it is not possible to resolve whether E-W extension in the Tibetan Plateau is triggered by the plate convection between India and Eurasia or is part of an adjustment to a change of boundary conditions in eastern Asia (Yin, 2000; Yin and Harrison, 2000).

We thus conclude that predominant, pervasive, and active E-W extension in the NW Indian Himalaya is a regional phenomenon and not restricted to the well-known regions of focused extension (e.g., Leo Pargil dome, the Gurla Mandhata dome, the Thakkola graben, the Ama Drime Massif, and the Yadong graben). Our observations demonstrate that E-W extension affects the entire mountain belt from the Indian-Eurasian suture zone to the footwall of the Main Central thrust in the Garhwal Himalaya. Importantly, extensional processes are not limited to regions north of the Southern Tibetan detachment system, as previously thought. Although geochronologic data documenting the onset of normal faulting are still sparse, E-W extension has apparently been a protracted process that started at around 16 Ma and has continued until the present day. Based on the regional relationships documented in our study, we propose that E-W extension in the NW Indian Himalaya is transferred from the Tibetan Plateau due to the inability of the Karakorum fault to accommodate all of the ongoing E-W extension on the Tibetan Plateau.

ACKNOWLEDGMENTS

We want to thank M.B. Bateman for providing the optically stimulated luminescence (OSL) data, Tashi Tsering for excellent logistical support, A. Yin, M. Murphy, and A. Webb for their constructive comments that helped to improve the paper, and K. Karlstrom for editorial support. This work was financially supported by the Deutsche Forschungsgemeinschaft (DFG) Graduate School 1364 at the University of Potsdam, Germany.

REFERENCES CITED

Aoya, M., Wallis, S., Terada, K., Lee, J., Kawakami, T., Wang, Y., and Heizler, M., 2005, North-south extension in the Tibetan crust triggered by granite emplacement: Geology, v. 33, no. 11, p. 853–856, doi: 10.1130/G21806.1.

Armijo, R., Tapponnier, P., Mercier, J.L., and Han, T.L., 1986, Quaternary extension in Southern Tibet—Field observations and tectonic implications: Journal of Geophysical Research, v. 91, no. B14, p. 13,803–13,872, doi: 10.1029/JB091iB14p13803.

Banerjee, D., Singhvi, A.K., Bagati, T.N., and Mohindra, R., 1997, Luminescence chronology of seismites at Sumdo (Spiti Valley) near Kaurik-Chango fault, northwestern Himalaya: Current Science, v. 73, no. 3, p. 276–281.

Banerjee, P., and Bürgmann, R., 2002, Convergence across the northwest Himalaya from GPS measurements: Geophysical Research Letters, v. 29, no. 13, doi: 10.1029/2002GL015184.

Bateman, M.D., and Catt, J.A., 1996, An absolute chronology for the raised beach deposits at Sewerby, E. Yorkshire, UK: Journal of Quaternary Science, v. 11, p. 389–395, doi: 10.1002/(SICI)1099-1417(199609/10)11:5<389::AID-JQS260>3.0.CO;2-K.

Beaumont, C., Jamieson, R.A., Nguyen, M.H., and Lee, B., 2001, Himalayan tectonics explained by extrusion of a low-viscosity crustal channel coupled to focused surface denudation: Nature, v. 414, p. 738–742, doi: 10.1038/414738a.

Bhargava, O.N., Ameta, S.S., Gaur, R.K., Kumar, S., Agarwal, A.N., Jalote, P.M., and Sadhu, M.L., 1978, The Kinnaur (H.P., India) earthquake of 19 January, 1975: Summary of geoseismological observations: Bulletin of the Indian Geological Association, v. 11, no. 1, p. 39–53.

Bookhagen, B., Thiede, R., and Strecker, M.R., 2005, Late Quaternary intensified monsoon phases control landscape evolution in the northwest Himalaya: Geology, v. 33, no. 2, p. 149–152, doi: 10.1130/G20982.1.

Buck, W.R., and Sokoutis, D., 1994, Analog model of gravitational collapse and surface extension during continental convergence: Nature, v. 369, no. 6483, p. 737–740, doi: 10.1038/369737a0.

Burchfiel, B.C., and Royden, L., 1985, North-South extension within the convergent Himalayan Region: Geology, v. 13, p. 679–682, doi: 10.1130/0091-7613(1985)13<679:NEWTCH>2.0.CO;2.

Burchfiel, B.C., Chen, Z., Royden, L.H., Liu, Y., and Deng, C., 1991, Extensional development of Gabo Valley, southern Tibet: Tectonophysics, v. 194, p. 187–193, doi: 10.1016/0040-1951(91)90283-X.

Burchfiel, B.C., Zhileng, C., Hodges, K.V., Yuping, L., Royden, L.H., Changrong, D., and Jiene, X., 1992, The South Tibetan detachment system, Himalayan orogen: Extension contemporaneous with and parallel to shortening in a collisional mountain belt: Geological Society of America Special Paper 269, p. 1–41.

Burg, J., Brunel, M., Gapais, D., Chen, G., and Liu, G., 1984, Deformation of leucogranites of the Crystalline Main Central sheet in southern Tibet (China): Bulletin of the Seismological Society of America, v. 6, no. 5, p. 535–542.

Burtman, V., and Molnar, P., 1993, Geological and geophysical evidence for deep subduction of continental crust beneath the Pamir: Geological Society of America Special Paper 281, 76 p.

Chen, W., and Yang, Z., 2004, Earthquakes beneath the Himalayas and Tibet: Evidence for strong lithospheric mantle: Science, v. 304, p. 1949–1952, doi: 10.1126/science.1097324.

Chevalier, M.-L., Fyerson, F.J., Tapponnier, P., Finkel, R.C., Van der Word, J., and Qing, L., 2005, Slip-rate measurements on the Karakorum fault imply secular variations in fault motion: Science, v. 307, p. 411–414, doi: 10.1126/science.1105466.

Cottle, J.M., Jessup, M.J., Newell, D.L., Horstwood, M.S.A., Noble, S.R., Parrish, R.R., Waters, D.J., and Searle, M.P., 2009, Geochronology of granulitized eclogite from the Ama Drime Massif: Implications for the tectonic evolution of the South Tibetan Himalaya: Tectonics, v. 28, doi: 10.1029/2008TC002256.

DiPietro, J.A., and Pogue, K.R., 2004, Tectonostratigraphic subdivisions of the Himalaya: A view from the west: Tectonics, v. 23, doi: 10.1029/2003TC001554.

England, P., and Houseman, G., 1989, Extension during continental convergence with application to the Tibetan Plateau: Journal of Geophysical Research, v. 94, no. B12, p. 17,561–17,579, doi: 10.1029/JB094iB12p17561.

Epard, J.-L., and Steck, A., 2008, Structural development of the Tso Morari ultra-high pressure nappe of the Ladakh Himalaya: Tectonophysics, v. 451, no. 1–4, p. 242–264, doi: 10.1016/j.tecto.2007.11.050.

Fuchs, G., and Linner, M., 1996, On the geology of the suture zone and Tso Morari dome in Easthern Ladakh (Himalaya): Jahrbuch für Geologischen Bundesanstalt, Vienna/A, v. 139, p. 191–207.

Gansser, A., 1964, Geology of the Himalayas: London, Interscience, 289 p.

Garzione, C.N., Dettman, D.L., Quade, J., DeCelles, P.G., and Butler, R.F., 2000, High times on the Tibetan Plateau: Paleoelevation of the Thakkhola graben, Nepal: Geology, v. 28, p. 339–342, doi: 10.1130/0091-7613(2000)28<339:HTOTTP>2.0.CO;2.

Garzione, C.N., DeCelles, P.G., Hodkinson, D., Ojha, R., and Upreti, B., 2003, E-W extension and Miocene environmental change in the Southern Tibetan Plateau: Thakkhola graben, central Nepal: Geological Society of America Bulletin, v. 115, no. 1, p. 3–20, doi: 10.1130/0016-7606(2003)115<0003:EWEAME>2.0.CO;2.

Grujic, D., Casey, M., Davidson, C., Hollister, L.S., Kundig, R., Pavlis, T., and Schmid, S., 1996, Ductile extrusion of the Higher Himalayan crystalline in Bhutan: Evidence from quartz microfabrics: Tectonophysics, v. 260, no. 1–3, p. 21–43, doi: 10.1016/0040-1951(96)00074-1.

Guo, L., Zhang, J., and Zhang, B., 2008, Structures, kinematics, thermochronology and tectonic evolution of the Ramba gneiss dome in the northern Himalaya: Progress in Natural Science, v. 18, p. 851–860, doi: 10.1016/j.pnsc.2008.01.016.

Harvard Global CMT Catalog, 2009, Centroid Moment Tensor Catalog: http://www.globalcmt.org/CMTsearch.html.

Hayden, H.H., 1904, The geology of Spiti with parts of Bushahr and Rupshu: Memoirs of the Geological Survey of India, v. 6, p. 1–121.

Hodges, K.V., Parrish, R.R., and Searle, M.P., 1996, Tectonic evolution of the Central Annapurna Range, Nepalese Himalayas: Tectonics, v. 15, p. 1264–1291, doi: 10.1029/96TC01791.

Hodges, K.V., Hurtado, J.M., and Whipple, K.X., 2001, Southward extrusion of Tibetan crust and its effect on Himalayan tectonics: Tectonics, v. 20, no. 6, p. 799–809, doi: 10.1029/2001TC001281.

Hurtado, J.M., Hogdes, K.V., and Whipple, K.X., 2001, Neotectonics of the Thakkhola graben and implications for recent activity on the South Tibetan fault system in the central Nepal Himalaya: Geological Society of America Bulletin, v. 113, no. 2, p. 222–240, doi: 10.1130/0016-7606(2001)113<0222:NOTTGA>2.0.CO;2.

Janda, C., Hager, C., Grasemann, B., Draganits, E., Vannay, J.-C., Bookhagen, B., and Thiede, R., 2002, The Karcham normal fault: Implications for an active extruding wedge, Sutlej Valley, NW Himalaya: Journal of Asian Earth Sciences, v. 20, p. 19–20.

Jessup, M.J., Newell, D.L., Cottle, J.M., Berger, A.L., and Spotila, J.A., 2008, Orogen-parallel extension and exhumation enhanced by denudation in the trans-Himalayan Arun River gorge, Ama Drime Massif, Tibet-Nepal: Geology, v. 36, no. 7, p. 587–590, doi: 10.1130/G24722A.1.

Kapp, P., and Guynn, J., 2004, Indian punch rifts Tibet: Geology, v. 32, no. 11, p. 993–996, doi: 10.1130/G20689.1.

Kapp, P.A., and Yin, A., 2001, Unbending of the lithosphere as a mechanism for active rifting in Tibet: Insight from elastic modelling: Eos (Transaction, American Geophysical Union), v. 82, no. 47, Fall meeting supplement, abstract no. T11E–0893.

Kayal, J., Kamble, V., and Rastogi, B.K., 2000, Aftershocks sequence of Uttarkashi earthquake of October 20, 1991: Geological Survey of India Special Publication 30, p. 203–217.

Kim, Y.-S., Peacock, D.C.P., and Sanderson, D.J., 2004, Fault damage zones: Journal of Structural Geology, v. 26, p. 503–517, doi: 10.1016/j.jsg.2003.08.002.

Klootwijk, C.T., Conaghan, P.J., and Powell, C.M., 1985, The Himalayan arc—Large-scale continental subduction, oroclinal bending and back-arc spreading: Earth and Planetary Science Letters, v. 75, no. 2–3, p. 167–183, doi: 10.1016/0012-821X(85)90099-8.

Lacassin, R., Valli, F., Arnaud, N., Leloup, P.H., Paquette, J.L., Haibing, L., Tapponnier, P., Chevalier, M.-L., Guillot, S., Maheo, G., and Zhiqin, X., 2004, Large-scale geometry, offset and kinematic evolution of the Karakorum fault, Tibet: Earth and Planetary Science Letters, v. 219, p. 255–269, doi: 10.1016/S0012-821X(04)00006-8.

Le Fort, M., Freytet, P., and Colchen, M., 1982, Structural and sedimentological evolution of the Thakkhola-Mustang graben (Nepal Himalayas): Zeitschrift für Geomorphologie, v. 42, p. 75–98.

McCaffrey, R., 1996, Estimates of modern arc-parallel strain rates in fore-arcs: Geology, v. 24, no. 1, p. 27–30, doi: 10.1130/0091-7613(1996)024<0027:EOMAPS>2.3.CO;2.

McCaffrey, R., and Nabelek, J., 1998, Role of oblique convergence in the active deformation of the Himalayas and southern Tibet Plateau: Geology, v. 26, p. 691–694, doi: 10.1130/0091-7613(1998)026<0691:ROOCIT>2.3.CO;2.

Meigs, A., Burbank, D., and Beck, R., 1995, Middle–late Miocene (>10 Ma) initiation of the Main Boundary thrust in the Western Himalaya: Geology, v. 23, p. 423–426, doi: 10.1130/0091-7613(1995)023<0423:MLMMFO>2.3.CO;2.

Michard, A., Chopin, C., and Henry, C., 1993, Compression versus extension in the exhumation of the Dora-Maira coesite-bearing unit, western Alps, Italy: Tectonophysics, v. 221, p. 173–193, doi: 10.1016/0040-1951(93)90331-D.

Middlemiss, C.S., 1910, The Kangra earthquake of 4th April, 1905: Geological Survey of India Memoir, v. 38, p. 1–409.

Mohindra, R., and Bagati, T.N., 1996, Seismically induced soft-sediment deformation structures (seismites) around Sumdo in the lower Spiti Valley (Tethys Himalaya): Sedimentary Geology, v. 101, no. 1–2, p. 69–83, doi: 10.1016/0037-0738(95)00022-4.

Molnar, P., 1984, Structure and tectonics of the Himalaya: Constraints and implications of geophysical data: Annual Review of Earth and Planetary Sciences, v. 12, p. 489–518, doi: 10.1146/annurev.ea.12.050184.002421.

Molnar, P., 1992, A review of seismicity, recent faulting and active deformation of the Tibetan Plateau: Journal of Himalayan Geology, v. 31, no. 1, p. 43–78.

Molnar, P., and Chen, W.P., 1983, Focal depths and fault plane solutions of earthquakes under the Tibetan Plateau: Journal of Geophysical Research, v. 88, no. B2, p. 1180–1196, doi: 10.1029/JB088iB02p01180.

Molnar, P., and Lyon-Caen, H., 1989, Fault-plane solutions of earthquakes and active tectonics of the Tibetan Plateau and its margins: Geophysical Journal International, v. 99, no. 1, p. 123–153, doi: 10.1111/j.1365-246X.1989.tb02020.x.

Molnar, P., and Tapponnier, P., 1978, Active tectonics of Tibet: Journal of Geophysical Research–B: Solid Earth, v. 83, p. 5361–5375, doi: 10.1029/JB083iB11p05361.

Murphy, M.A., and Burgess, W., 2006, Geometry, kinematics, and landscape characteristics of an active transtension zone, Karakorum fault system, southwest Tibet: Journal of Structural Geology, v. 28, p. 268–283, doi: 10.1016/j.jsg.2005.10.009.

Murphy, M.A., and Copeland, P., 2005, Transtensional deformation in the Central Himalaya and its role in accommodating growth of the Himalayan orogen: Tectonics, v. 24, doi: 10.1029/2004TC001659.

Murphy, M.A., Saylor, J.E., and Ding, L., 2009, Late Miocene topographic inversion in southwest Tibet based on integrated paleoelevation reconstructions and structural history: Earth and Planetary Science Letters, v. 282, p. 1–9, doi: 10.1016/j.epsl.2009.01.006.

Murphy, M.A., Yin, A., Kapp, P., Harrison, T.M., Lin, D., and Jinghui, G., 2000, Southward propagation of the Karakoram fault system, southwest Tibet: Timing and magnitude of slip: Geology, v. 28, no. 5, p. 451–454, doi: 10.1130/0091-7613(2000)28<451:SPOTKF>2.0.CO;2.

Murphy, M.A., Yin, A., Kapp, P., Harrison, T.M., Manning, C.E., Ryerson, F.J., Ding, L., and Guo, J.H., 2002, Structural evolution of the Gurla Mandhata detachment system, southwest Tibet: Implications for the eastward extent of the Karakoram fault system: Geological Society of America Bulletin, v. 114, no. 4, p. 428–447, doi: 10.1130/0016-7606(2002)114<0428:SEOTGM>2.0.CO;2.

Murray, A.S., and Wintle, A.G., 2000, Luminescence dating of quartz using an improved single-aliquot regenerative-dose protocol: Radiation Measurements, v. 32, p. 57–73, doi: 10.1016/S1350-4487(99)00253-X.

NEIC, 2009, National Earthquake Information Center (NEIC) Catalog of Global Seismicity: http://neic.usgs.gov/neis/epic/.

Nelson, K.D., Zhao, W.J., Brown, L.D., Kuo, J., Che, J.K., Liu, X.W., Klemperer, S.L., Makovsky, Y., Meissner, R., Mechie, J., Kind, R., Wenzel, F., Ni, J., Nabelek, J., Chen, L.S., Tan, H.D., Wei, W.B., Jones, A.G., Booker, J., Unsworth, M., Kidd, W.S.F., Hauck, M., Alsdorf, D., Ross, A., Cogan, M., Wu, C.D., Sandvol, E., and Edwards, M., 1996, Partially molten middle crust beneath southern Tibet: Synthesis of project INDEPTH results: Science, v. 274, no. 5293, p. 1684–1688, doi: 10.1126/science.274.5293.1684.

Neumayer, J., Wiesmayr, G., Janda, C., Grasemann, B., and Draganits, E., 2004, Eohimalayan fold and thrust belt in the NW-Himalaya (Lingti-Pin Valleys): Shortening and depth to detachment calculation: Australian Journal of Earth Sciences, v. 95/96, p. 28–36.

Ni, J., and Barazangi, M., 1984, Seismotectonics of the Himalayan collision zone—Geometry of the underthrusting Indian plate beneath the Himalaya: Journal of Geophysical Research, v. 89, no. B2, p. 1147–1163, doi: 10.1029/JB089iB02p01147.

Ortner, H., Reiter, F., and Acs, P., 2002, Easy handling of tectonic data: The programs TectonicVB for Mac and TectonicsFP for Windows: Computers & Geosciences, v. 28, p. 1193–1200, doi: 10.1016S0098-3004(02)00038-9.

Pandey, M., Tandukar, R., Avouac, J., Vergne, J., and Héritier, T., 1999, Seismotectonics of the Nepal Himalaya from a local seismic network: Journal of Asian Earth Sciences, v. 17, p. 703–712, doi: 10.1016S1367-9120(99)00034-6.

Peltzer, G., and Tapponnier, P., 1988, Formation and evolution of strike-slip faults, rifts and basins during the India-Asia collision: An experimental approach: Journal of Geophysical Research, v. 93, p. 15,095–15,117.

Phillips, R.J., Parrish, R.R., and Searle, M.P., 2004, Age constraints on ductile deformation and long-term slip rates along the Karakorum fault zone, Ladakh: Earth and Planetary Science Letters, v. 226, p. 305–319, doi: 10.1016/j.epsl.2004.07.037.

Rastogi, B.K., 2000, Chamoli earthquake of magnitude 6.6 on 29 March 1999: Journal of the Geological Society of India, v. 55, p. 505–515.

Ratschbacher, L., Frisch, W., Liu, G.H., and Chen, C.S., 1994, Distributed deformation in southern and western Tibet during and after the India-Asia collision: Journal of Geophysical Research–Solid Earth, v. 99, no. B10, p. 19,917–19,945, doi: 10.1029/94JB00932.

Robinson, A.C., Yin, A., Manning, C.E., Harrison, T.M., Zhang, S., and Wang, X., 2007, Cenozoic evolution of the eastern Pamir: Implications for strain-accommodation mechanisms at the western end of the Himalayan-Tibetan orogen: Geological Society of America Bulletin, v. 119, no. 7/8, p. 882–896, doi: 10.1130/B25981.1.

Royden, L.H., and Burchfiel, B.C., 1987, Thin-skinned north-south extension within the convergent Himalayan region: Gravitational collapse of a Miocene topographic front, *in* Coward, M.P., Dewey, J.F., and Hancock, P.L., eds., Continental extensional tectonics: Geological Society of London Special Publication 28, p. 611–619, doi: 10.1144/GSL.SP.1987.028.01.40.

Saylor, J., Quade, J., Dettman, D.L., DeCelles, P., Kapp, P., and Ding, L., 2009, The late Miocene through Present paleoelevation history of southwestern Tibet: American Journal of Science, v. 309, p. 1–42, doi: 10.2475/01.2009.01.

Searle, M.P., and Phillips, R.J., 2007, Relationships between right-lateral shear along the Karakoram fault and metamorphism, magmatism, exhumation and uplift: Evidence from the K2-Gasherbrum-Pangong Ranges, north Pakistan and Ladakh: Journal of the Geological Society of London, v. 164, p. 439–450, doi: 10.1144/0016-76492006-072.

Searle, M.P., Weinberg, R.F., and Dunlap, W.J., 1998, Transpressional tectonics along the Karakoram fault zone, northern Ladakh: Constraints on Tibetan extrusion, *in* Holdsworth, R.E., Strachan, R.A., and Dewey, J.F., eds., Continental Transpressional and Transtensional Tectonics: Geological Society of London Special Publication 135, p. 307–326.

Seeber, L., and Armbruster, J., 1981, Great detachment earthquakes along the Himalayan arc and the long-term forecasts, *in* Simpson, E., and Richards, P., eds., Earthquake Prediction: An International Review: Washington, D.C., American Geophysical Union, Maurice Ewing Series, v. 4, p. 259–277.

Seeber, L., and Armbuster, J., 1984, Some elements of continental subduction along the Himalayan front: Tectonophysics, v. 105, p. 263–278, doi: 10.1016/0040-1951(84)90207-5.

Selverstone, J., 2005, Are the Alps collapsing?: Annual Review of Earth Sciences, v. 33, p. 2.1–2.20.

Seward, D., and Mancktelow, N., 1994, Neogene kinematics of the central and western Alps: Evidence from fission-track dating: Geology, v. 22, no. 9, p. 803–806, doi: 10.1130/0091-7613(1994)022<0803:NKOTCA>2.3.CO;2.

Singh, S., Sinha, P., Jain, A.K., Singh, V.N., and Srivastava, L.S., 1975, Preliminary report on the January 19,

1975, Kinnaur earthquake in Himachal Pradesh: Earthquake Engineering Studies, v. 75, no. 4, p. 1–32.

Spang, J., 1972, Numerical method for dynamic analysis of calcite twin lamellae: Geological Society of America Bulletin, v. 83, p. 467–472, doi: 10.1130/0016-7606(1972)83[467:NMFDAO]2.0.CO;2.

Sperner, B., 1996, Computer programs for the kinematic analysis of brittle deformation structures and the Tertiary tectonic evolution of the Western Carpathians Slovakia: Tübinger Geowissenschaftliche Arbeiten, v. A 27, 120 p.

Steck, A., Spring, L., Vannay, J.-C., Masson, H., Bucher, H., Stutz, E., Marchant, R., and Tieche, J.-C., 1993, The tectonic evolution of the northwestern Himalaya in eastern Ladakh and Lahul, India, *in* Treloar, P.J., and Searle, M.P., eds., Himalayan Tectonics: Geological Society of London Special Publication 74, p. 265–276.

Strecker, M., Frisch, W., Hamburger, M.W., Ratschbacher, L., Semiletkin, S., Zamoruyev, A., and Sturchio, N., 1995, Quaternary deformation in the Eastern Pamirs, Tadzhikistan and Kyrgyzstan: Tectonics, v. 14, p. 1061–1079, doi: 10.1029/95TC00927.

Sue, C., Delacou, B., Champagnac, J.-D., Allanic, C., and Burkhard, M., 2007, Aseismic deformation in the Alps: GPS vs. seismic strain quantification: Terra Nova, v. 19, p. 182–188, doi: 10.1111/j.1365-3121.2007.00732.x.

Tapponnier, P., and Molnar, P., 1976, Slip-line field-theory and large-scale continental tectonics: Nature, v. 264, no. 5584, p. 319–324, doi: 10.1038/264319a0.

Tapponnier, P., Peltzer, G., Ledain, A., Armijo, R., and Cobbold, P., 1982, Propagating extrusion tectonics in Asia, new insights from simple experiments with plasticine: Geology, v. 10, no. 12, p. 611–616, doi: 10.1130/0091-7613(1982)10<611:PETIAN>2.0.CO;2.

Taylor, M., Yin, A., Ryerson, F.J., Kapp, P., and Ding, L., 2003, Conjugate strike-slip faulting along the Bangong-Nujiang suture zone accommodates coeval east-west extension and north-south shortening in the interior of the Tibetan Plateau: Tectonics, v. 22, no. 4, doi: 10.1029/2002TC001361.

Thiede, R., Arrowsmith, J.R., Bookhagen, B., McWilliams, M., Sobel, E., and Strecker, M., 2005, From tectonically to erosionally controlled development of the Himalayan orogen: Geology, v. 33, no. 8, p. 689–692, doi: 10.1130/G21483.1.

Thiede, R., Arrowsmith, J.R., Bookhagen, B., McWilliams, M., Sobel, E., and Strecker, M., 2006, Dome formation and extension in the Tethyan Himalaya, Leo Pargil, northwest India: Geological Society of America Bulletin, v. 118, p. 635–650, doi: 10.1130/B25872.1.

Turner, F., 1953, Nature and dynamic interpretation of deformation lamellae in calcite of three marbles: American Journal of Science, v. 251, p. 276–298.

Vannay, J.-C., and Grasemann, B., 1998, Inverted metamorphism in the High Himalaya of Himachal Pradesh (NW India): Phase equilibria versus thermobarometry: Schweizerische Mineralogische und Petrographische Mitteilungen, v. 78, p. 107–132.

Vannay, J.-C., and Grasemann, B., 2001, Himalayan inverted metamorphism and syn-convergence extension as a consequence of a general shear extrusion: Geological Magazine, v. 138, no. 3, p. 253–276, doi: 10.1017/S0016756801005313.

Vannay, J.-C., Grasemann, B., Rahn, M., Frank, W., Carter, A., Baudraz, V., and Cosca, M., 2004, Miocene to Holocene exhumation of metamorphic crustal wedges in the NW Himalaya: Evidence for tectonic extrusion coupled to fluvial erosion: Tectonics, v. 23, doi: 10.1029/2002TC001429.

Webb, A.G., Yin, A., Harrison, T.M., Célérier, J., and Burgess, W.P., 2007, The leading edge of the Greater Himalayan Crystalline complex revealed in the NW Indian Himalaya: Implications for the evolution of the Himalayan orogen: Geology, v. 35, no. 10, p. 955–958, doi: 10.1130/G23931A.1.

Wesnousky, S., Kumar, S., Mohindra, R., and Thakur, V., 1999, Uplift and convergence along the Himalayan Frontal thrust of India: Tectonics, v. 18, no. 6, p. 967–976, doi: 10.1029/1999TC900026.

Wheeler, J., and Butler, R., 1993, Evidence for extension in the western Alpine orogen: The contact between the oceanic Piemonte and overlying continental Sesia units: Earth and Planetary Science Letters, v. 117, p. 457–474, doi: 10.1016/0012-821X(93)90097-S.

Wiesmayr, G., and Grasemann, B., 2002, Eohimalayan fold and thrust belt: Implications for the geodynamic evolution of the NW-Himalaya (India): Tectonics, v. 21, no. 6, doi: 10.1029/2002TC001363.

Wu, C., Nelson, K., Wortman, G., Samson, S., Yue, Y., Li, J., Kidd, W., and Edwards, M., 1998, Yadong cross structure and South Tibetan detachment in the east central Himalaya (89–90°E): Tectonics, v. 17, p. 28–45, doi: 10.1029/97TC03386.

Yin, A., 1989, Origin of regional, rooted low-angle normal faults: A mechanical model and its tectonic implications: Tectonics, v. 8, no. 3, p. 469–482, doi: 10.1029/TC008i003p00469.

Yin, A., 2000, Mode of Cenozoic east-west extension in Tibet suggesting a common origin of rifts in Asia during the Indo-Asian collision: Journal of Geophysical Research, v. 105, no. B9, p. 21,745–21,759.

Yin, A., 2006, Cenozoic tectonic evolution of the Himalayan orogen as constrained by along-strike variation of structural geometry, exhumation history, and foreland sedimentation: Earth-Science Reviews, v. 76, no. 1–2, p. 1–131, doi: 10.1016/j.earscirev.2005.05.004.

Yin, A., and Harrison, T.M., 2000, Geological evolution of the Himalayan-Tibetan orogen: Annual Review of Earth and Planetary Sciences, v. 28, p. 211–280, doi: 10.1146/annurev.earth.28.1.211.

Zhang, P., Shen, Z., Wang, M., Gan, W., Bürgmann, R., Molnar, P., Wang, Q., Niu, Z., Sun, J., Wu, J., Hanrong, S., and Xinzhao, Y., 2004, Continuous deformation of the Tibetan Plateau from Global Positioning System data: Geology, v. 32, no. 9, p. 809–812, doi: 10.1130/G20554.1.

Manuscript Received 1 December 2008
Revised Manuscript Received 1 June 2009
Manuscript Accepted 1 July 2009

Printed in the USA